Master Thesis, Department of Geosciences

Petrographic evaluation of the Middle Jurassic sandstones of the Brent Group, North Sea

A petrographic study of the Ness, Etive and Rannoch formations

Per Christian Ekre

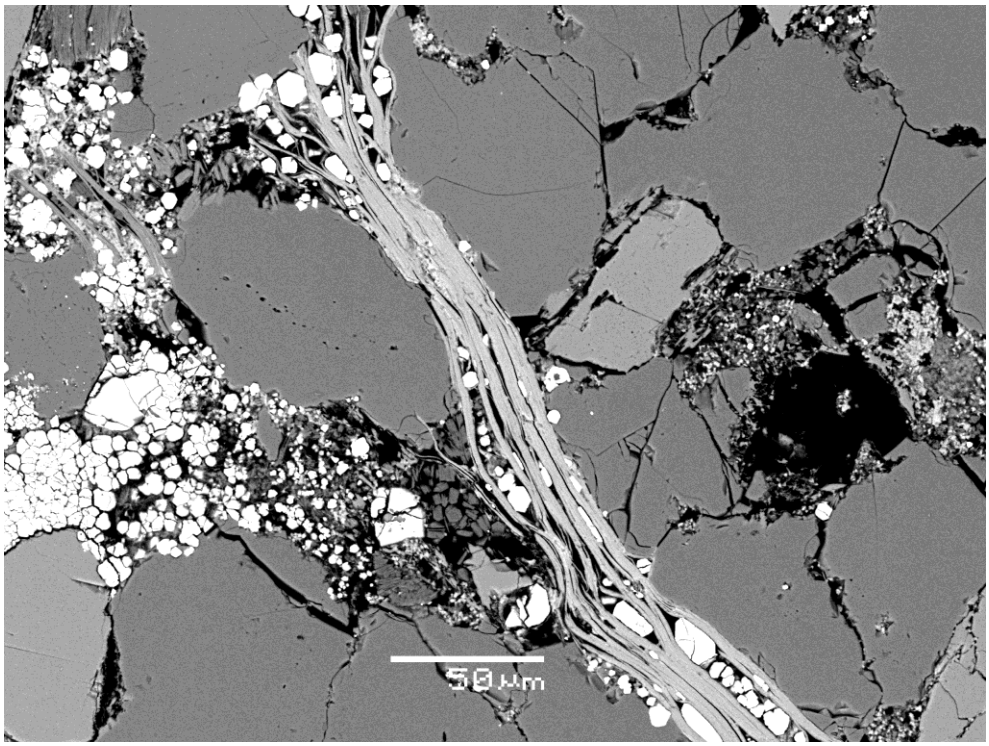

UNIVERSITY OF OSLO

FACULTY OF MATHEMATICS AND NATURAL SCIENCES

Petrographic evaluation of the Middle Jurassic sandstones of the Brent Group, North Sea

A petrographic study of the Ness, Etive and Rannoch formations

Per Christian Ekre

Master Thesis in Geosciences

Discipline: Geology

Department of Geosciences

Faculty of Mathematics and Natural Sciences

University of Oslo

11.01.2015

Abstract

Quartz cementation and precipitation of clays are two of the most porosity and permeability reducing processes in the Brent Group sediments. Dissolved feldspar and authigenic kaolinite occur at shallow depths as a function of pore-water flow and pore-water chemistry. No significant increase of secondary porosity with depth is shown to occur. Petrographic analyses of the Ness, Etive and Rannoch formations show a reduction of K-feldspar with depth. This can be explained by dissolution of K-feldspars during illitization of kaolinite at temperatures exceeding 130°C (>3.5 km) and albitization of K-feldspars at depths between 2.5 and 3.5 km. Petrographic analyses have also shown that the amount of feldspar and kaolinite and their ratio are controlled by depositional environments. In deeply buried sandstones (>3.5 km), quartz cementation and illitization of kaolinite are the two most porosity and permeability damaging processes. Small amounts of illite are also observed in sandstones at temperatures around 70°C. This can partly be explained by infiltration of some smectite into channel sandstones due to flooding of the delta plain.

Carbonate cementation occur at shallow depths and can be very damaging with respect to porosity. Extensive carbonate cementation is in literature mainly linked to marine facies. However, thin layers of extensive carbonate cement are also observed in the more fluvial delta plain environment of the Ness Formation. This suggests that fluid barriers formed by carbonate cementation should not be disregarded in non-marine facies.

Acknowledgements

I would like to thank my supervisors Professor Jens Jahren and Professor Knut Bjørlykke for valuable discussions and feedback. Their expertise and interest in diagenesis and related topics have been of great importance and inspiration. They truly rock.

In addition, I would like to give thanks to Senior Engineer Berit Løken Berg for tutoring me in scanning electron microscopy. I would also like to thank Oluwakemi Yetunde Ogebule for her help.

The time spent during this master's degree would not have been the same without my fellow students and friends at ZEB. Our discussions and laughs are truly appreciated. I wish you all the best.

Lastly, I would like to give a shout out to my family and friends for great support. I am most grateful.

January 2015

Per Christian Ekre

Table of Contents

1 Introduction

1.1 Purpose and methods

The aim for this study is to investigate how mineral assemblages and facies in the Ness, Rannoch and Etive formations impact porosity, permeability and intergranular volume at various temperatures and depths (1.8 km - 4.3 km). Petrographic analyses of 55 thin sections using an optical microscope and a scanning electron microscope were performed.

1.2 Study area

A number of thin sections collected from wells located within certain oil and gas fields of the Tampen area were investigated. A more detailed description of wells and fields is given in chapter 3.

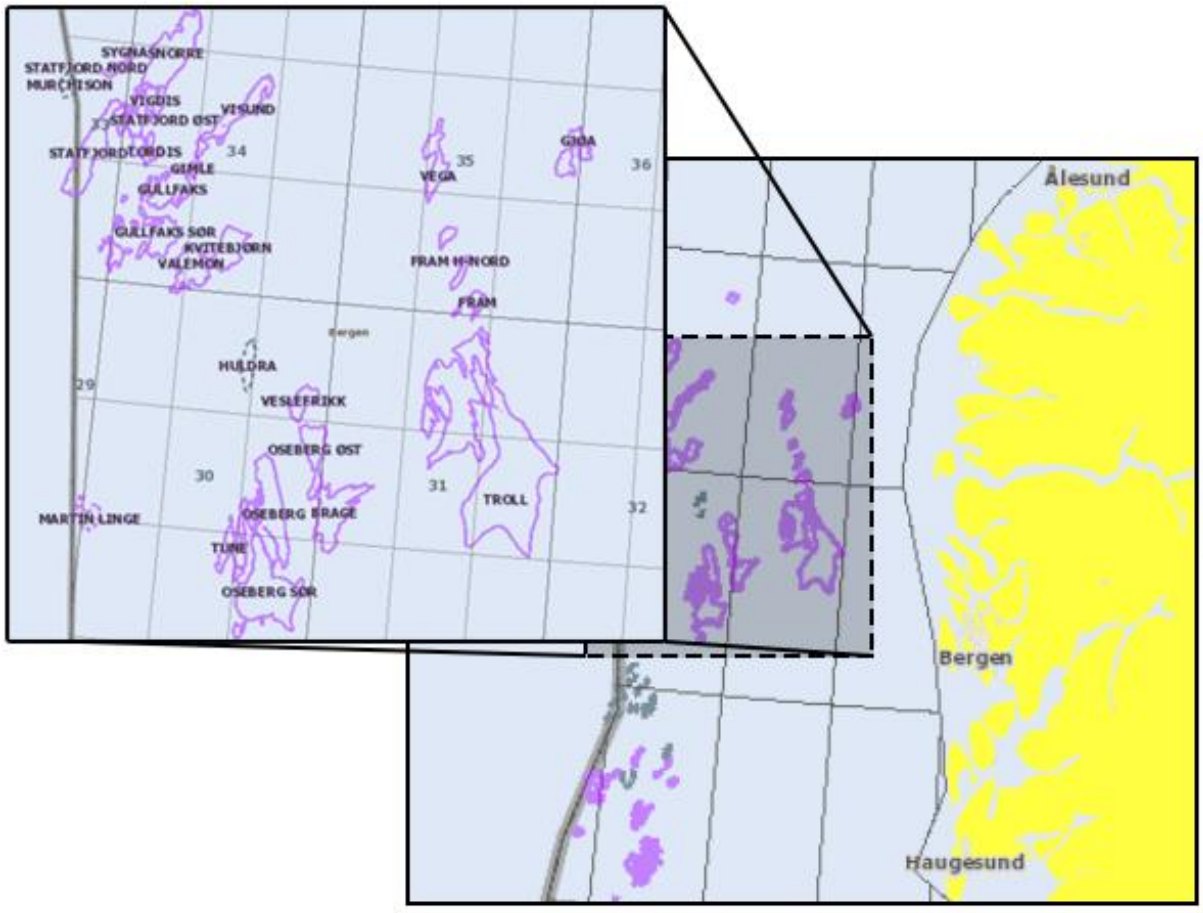

Figure 1.1: Map of the studied area, modified from npd.no (2014).

2 Diagenesis of sedimentary rocks

2.1 Introduction

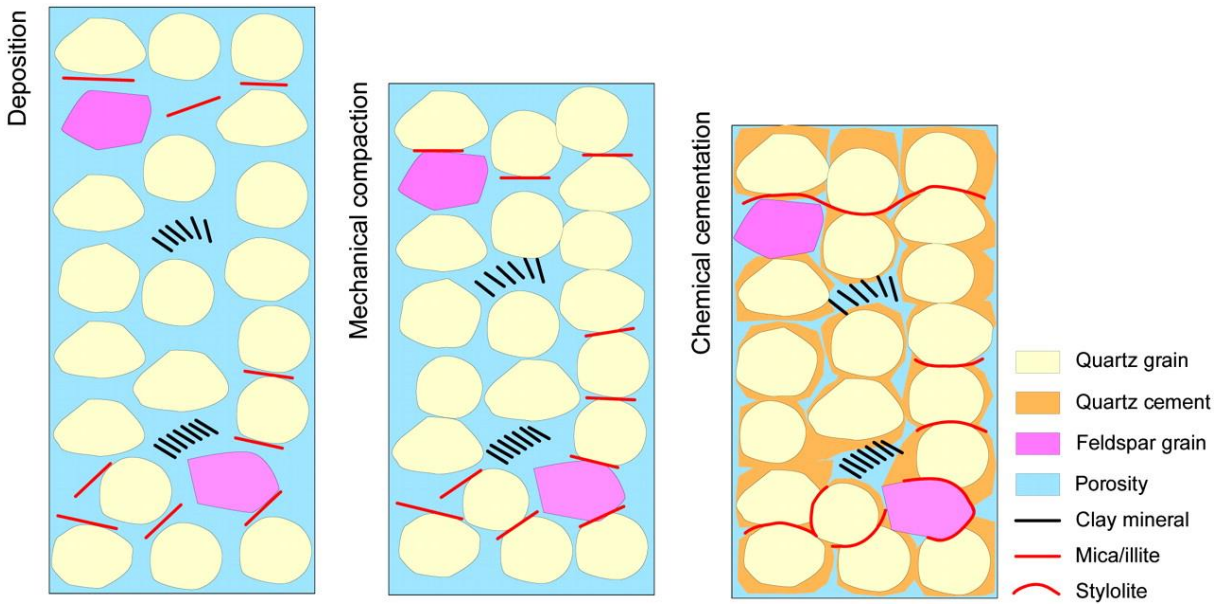

Figure 2.1: Illustration of the different processes during the diagenesis of sandstones (GeoscienceWorld, 2014)

Diagenesis includes all the changes of the sediments from deposition up to the moment of metamorphism. We can view diagenesis as a group of processes driven by different factors. The main processes of diagenesis are mechanical compaction and chemical compaction (including cementation). As long as there is sediment influx into a basin, the overburden of the underlying sediments will continue to increase. The compaction strengthens the rock to withhold the stress caused by the overburden, which generally leads to a reduction of porosity. This chapter is mainly based on Bjørlykke and Jahren (2010), *Sandstones and sandstone reservoirs.*

2.2 Early diagenesis (<80°C)

Right after deposition the sediments has the highest potential to change their primary composition. While shallowly buried, the sediments may react to the atmosphere or water, as fluid flow and diffusion. The mineral assemblage present in the sediments has significant effect on porosity at greater depths. The composition of minerals may be altered as a result of meteoric water flow, which normally is under saturated in respect to the deposited minerals. This, along with oxidization, is the main contributors of weathering during early diagenesis.

However, the extent of weathering is not the same in different depositional environments (e.g. continental, lake, sea), because of the unequal distribution and access of groundwater and oxygen.

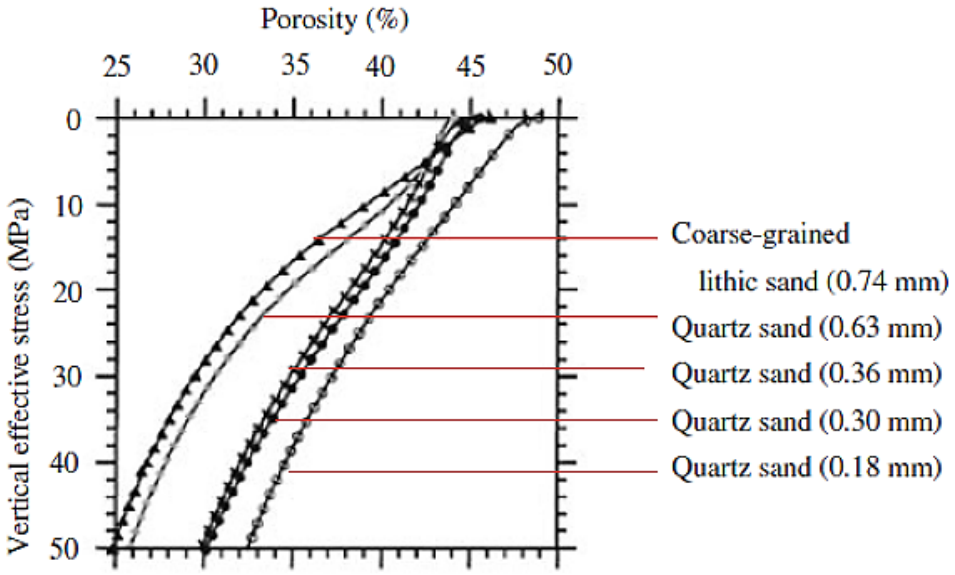

Figure 2.1: Porosity loss at depth as a function of initial grain size (Chuhan et al., 2003).

2.2.1 Feldspar dissolution and precipitation of kaolinite

Meteoric water is precipitated rainwater which has infiltrated the ground. Rainwater reacts with carbon dioxide (CO_2) and sulphur dioxide (SO_2) in the atmosphere, making it slightly acidic. This produces carbonic (H_2CO_3) and sulphuric acid (H_2SO_4). As long as the ground water table is above sea level, the meteoric water will seep through the beds with the highest permeability and into the basin. There it will react with the deposited carbonates, micas and feldspars and dissolve them. Decaying organic matter in the ground also releases carbon dioxide, contributing to more acidic water, hastening the weathering process. With time the meteoric water will reach equilibrium with the present minerals. This happens first with the carbonates, and later with the silicate minerals. Silicate minerals dissolve at a much slower rate compared to carbonates, so the porewater may remain under- or supersaturated with respect to silicates for a long time. Simply put, the reaction for precipitation of clay minerals is: rock (feldspar, mica) + water = clay (kaolinite, smectite) + cations (Velde, 1995).

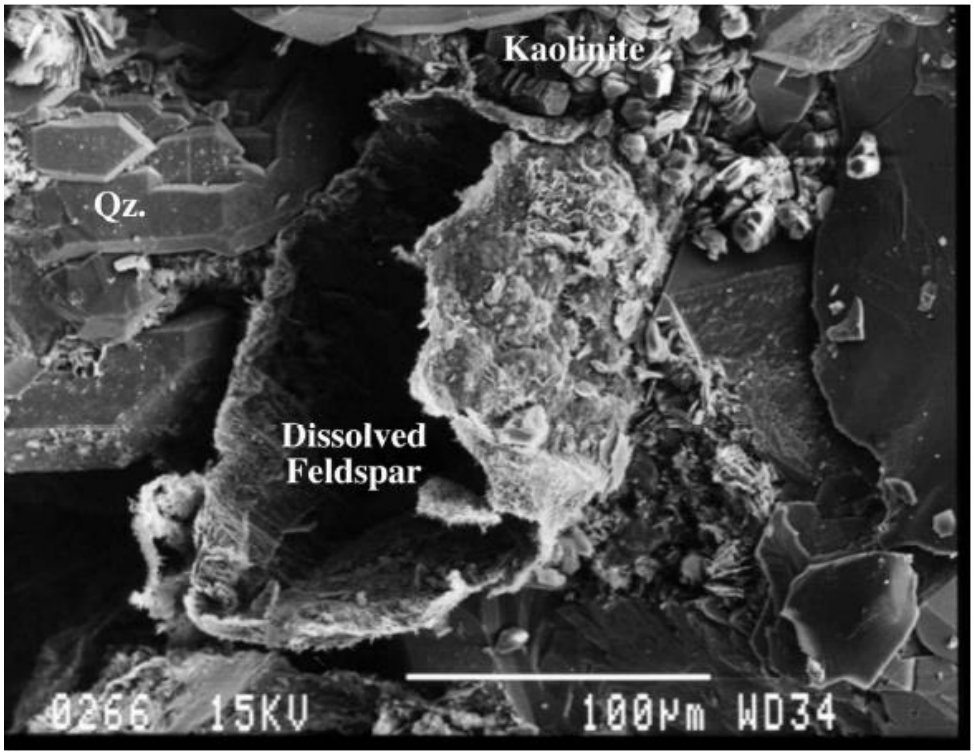

Figure 2.2: Shows dissolving feldspar and precipitation of kaolinite during early diagenesis in the Brent Group (Ness Fm.). Secondary porosity is made due to the dissolving feldspar, but lost again due to the precipitation of kaolinite. From (Bjørlykke, 1998).

The rates of precipitation of kaolinite and leaching of minerals are functions of the flux of groundwater flowing through each rock volume per unit of time.

The specific reactions of dissolving feldspar and muscovite, and precipitation of kaolinite:

Formula 2.1: A) Dissolution of feldspar and precipitation of kaolinite. B) Dissolution of muscovite and precipitation of kaolinite. After Bjørlykke and Aagaard (1992).

A) $$\underset{\text{Feldspar}}{2K(Na)AlSi_3O_8} + 2H^+ + 9H_2O = \underset{\text{Kaolinite}}{Al_2Si_2O_5(OH)_4} + \underset{\text{dissolved silica}}{4H_4SiO_4} + \underset{\text{dissolved cations}}{2K^+(2Na^+)}$$

B) $$\underset{\text{Muscovite}}{2KAl_3Si_3O_{10}(OH)_2} + 2H^+ + 3H_2O = \underset{\text{Kaolinite}}{3Al_2Si_2O_5(OH)_4} + 2K^+$$

The precipitated clay minerals become unstable at greater depths and higher temperatures, resulting in dissolution. This is sometimes referred to as reversed weathering: clay (kaolinite, smectite) + cations = illite + quartz + water (Velde, 1995).

The precipitation of kaolinite is also determined by other factors than meteoric water flow. If the pore-water is oversaturated with silica, or the K^+/H^+ ratio is too high the kaolinite will become unstable. Pore-water with too much dissolved silica will lead to precipitation of smectite rather than kaolinite. This occurs, however, mainly in arid environments and is likely not the case in the humid climate of the Middle Jurassic. Gibbsite may precipitate in exceptionally well flushed depositions.

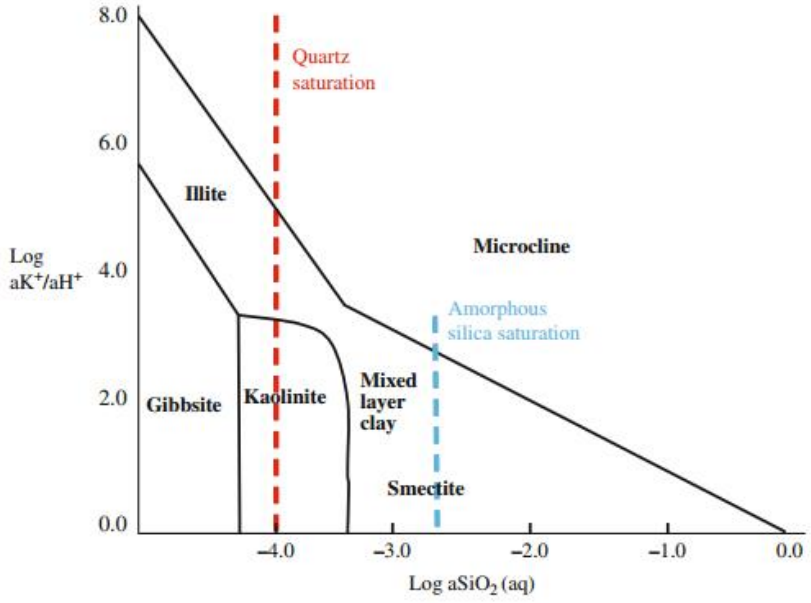

Figure 2.3: Diagram showing the stability of some minerals as a function of silica and the K+/H+ ratio (after Aagaard and Helgeson (1982)).

2.2.2 Mechanical compaction

During burial the sediments undergoes increasing stresses because of the growing overburden, and as a response we get mechanical compaction. The weight of the overburden forces the grains closer together, decreasing porosity. Further the mechanical strength is increased as a result of grain deformation and fracturing. The initial composition is still important as sorting, size, shape and minerals influence the mechanical compaction. It is also important to keep in mind that overpressure effectively decreases effective pressure. Mechanical compaction is important because it determines the intergranular volume (IGV), which is the porosity prior to cementation.

2.2.3 Carbonate cementation

In reservoir sandstones carbonate cementation is particularly interesting, because a carbonate cemented layer may act as a barrier, blocking liquids from further migration (Bjørlykke et al., 1992). Carbonates are subject to both mechanical and chemical compaction However, it differentiates from silicates in that carbonate reactions happens much faster, particularly at low temperatures. This may cause carbonate dissolution and cementation at shallow depths (Bjørlykke, 2013), indicating that stress is a more important factor than temperature. Carbonate grains or fossils originates from different sources and may be composed of different minerals (Bjørlykke, 2013, Moore, 1989). Generally, freshly deposited carbonates will be unstable and driven towards a more thermodynamically stable mineral structure (Moore, 1989). For example, high Mg-calcite and aragonite will try to alter or recrystallize, or may even be dissolved, in the process of stabilization. In the event of dissolution during freshwater flow, the net porosity may increase as a result. The meteoric water will however rapidly reach an equilibrium with respect to carbonate minerals, thus restricting the potential for net secondary porosity. Because carbonates forms into hard rock close to the surface the sediments will rather quickly become mechanically overconsolidated, meaning that it may be unable to undergo further mechanical compaction, even in deeply buried sandstones (> 4 km) (Bjørlykke, 2010).

Porosity loss in carbonates is still poorly understood. When compared, a carbonate reservoir will generally have lower porosity than a sandstone reservoir at the same depth (Bjørlykke, 2010).

The time of cementation may have an impact on porosity. If the content of aragonite is high, the compaction and cementation will happen sooner after burial. This is a result of the instability of aragonite crystals. If the porosity loss happens early during the diagenesis, it may help preserve the porosity at greater depths due to dissolution (Bjørlykke, 2010).

2.3 Intermediate burial

Mechanical and chemical compaction is separated by a transition zone, which is temperature dependent and occurs at roughly 70°C. While effective stresses drive the mechanical compaction, the chemical compaction processes are driven by reaction kinetics, where temperature is the most important factor. The second law of thermodynamics applies, as the mineral assembly is pushing towards thermodynamic equilibrium. In the case of siliciclastic minerals, this process is rather slow and highly temperature dependent. Intermediate burial marks the onset of quartz cementation which further stabilizes the sediment package.

2.3.1 Albitization of K-feldspar

The albitization of detrital potassium feldspars is an important process which may have a significant impact on reservoir quality (Saigal et al., 1988). In this process several changes to the sandstone may occur: alternation of the original sandstone framework composition; formation of by-products (e.g. illite, kaolinite and calcite); and pore size and geometry changes (Saigal et al., 1988). A study of the Brent Group Jurassic sandstones, done by Bjørlykke et al. (1992), shows there is little albitization in its shallow sandstones (< 2 km). Some partly albitized K-feldspar where found in samples at greater depths. XRD analyses done during this study shows depletion of K-feldspar in sample depths between 2.5 and 3.7 km.

Formula 2.2: Albitization of K-feldspar. After Saigal et al. (1988).

$$KAlSi_3O_8 + Na^+ \rightarrow NaAlSi_3O_8 + K^+$$

Albitization of K-feldspars starts at about 65°C and is completed by 120°C (Aagaard et al., 1990, Saigal et al., 1988).

2.4 Deep burial (>130°C)

During deep burial the sandstone is further cemented. Although quartz cementation starts at lower temperatures, it is during deep burial that the precipitation of quartz cement has the most profound effect on porosity. Besides quartz cementation, illitization of kaolinite starts at temperatures above 130°C. Illitization has a considerable effect on permeability.

2.4.1 Precipitation of illite

In most basins we find that porosity and permeability is highly reduced in deeply buried sandstones (3-3.5 km to 4-4.5 km). This is commonly due to quartz cementation (porosity) and precipitation of illite (permeability). While the much coarser kaolinite grains are deposited near deltas or the coastline, the much finer illite and chlorite grains may be transported further and tend to be more abundant in more distal facies (Weaver, 1989). Illite in deeply buried sandstones is normally formed diagenetically. Authigenic illite often occurs as fibrous crystals, filling the pore space in sandstones that either is or has been buried to a depth corresponding to temperatures > 120°C (Bjørlykke, 1998). This has a profound effect on permeability by greatly reducing it (Bjørlykke et al., 1992). In the North Sea, illite is normally precipitated at depths > 3.5 km at the expense of kaolin (Bjørlykke et al., 1992, Ehrenberg and Nadeau, 1989):

Formula 2.3: Dissolution of K-feldspar and kaolinite, and precipitation of illite and quartz. After Bjørlykke and Jahren (2010).

$$\underset{\text{K-feldspar}}{KAlSi_3O_8} + \underset{\text{Kaolinite}}{Al_2Si_2O_5(OH)_4} \rightarrow \underset{\text{Illite}}{KAl_3Si_3O_{10}(OH)_2} + \underset{\text{Quartz}}{2SiO_{2(aq)}} + H_2O \quad (2)$$

Illite may also be formed diagenetically by alteration of smectite, in temperatures ranging from 80-110°C (Eslinger and Pevear, 1988). The content of diagenetically formed illite and smectite in the shallowest (1.8 km) Brent sandstone reservoirs is very small (Bjørlykke et al., 1992). However, even though illitization of kaolinite is common in deeply buried sandstones, it is not uncommon to observe kaolinite in coexistence with feldspars in partly illitized sandstones at 3-4 km (Ehrenberg, 1991, Lanson et al., 2002). Lanson et al. (2002) therefore

concludes that temperature and illitization intensity seem to have no apparent relation. This will be further discussed in this study.

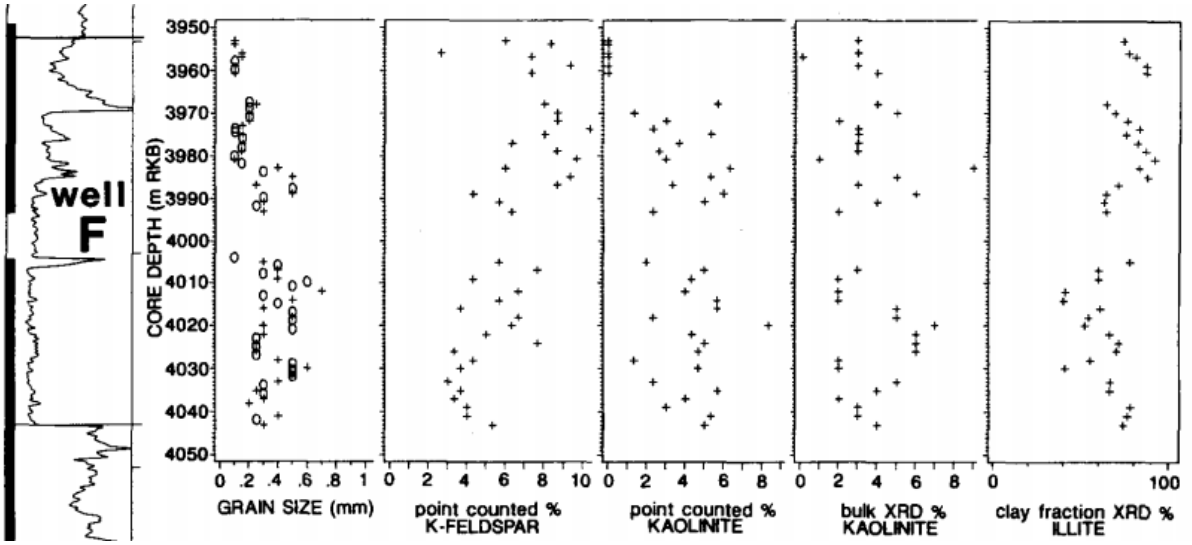

Figure 2.4: An example of coexisting kaolinite, feldspar and illite at depths up to 4 km. From a well in the Garn Formation, Haltenbanken, North Sea. (Ehrenberg, 1991).

Illite crystals change morphology with increasing paleo-burial depth (Lanson et al., 2002). At shallower depths (~3 km) the illite crystals are elongated and nearly one-dimensional (Lanson et al., 2002). With increasing depths the illite crystals tend to have a more rigid lath morphology (Lanson et al., 2002). Below 4 km, the illite crystals may in some cases have an isometric pseudo-hexagonal-shaped morphology (Lanson et al., 2002).

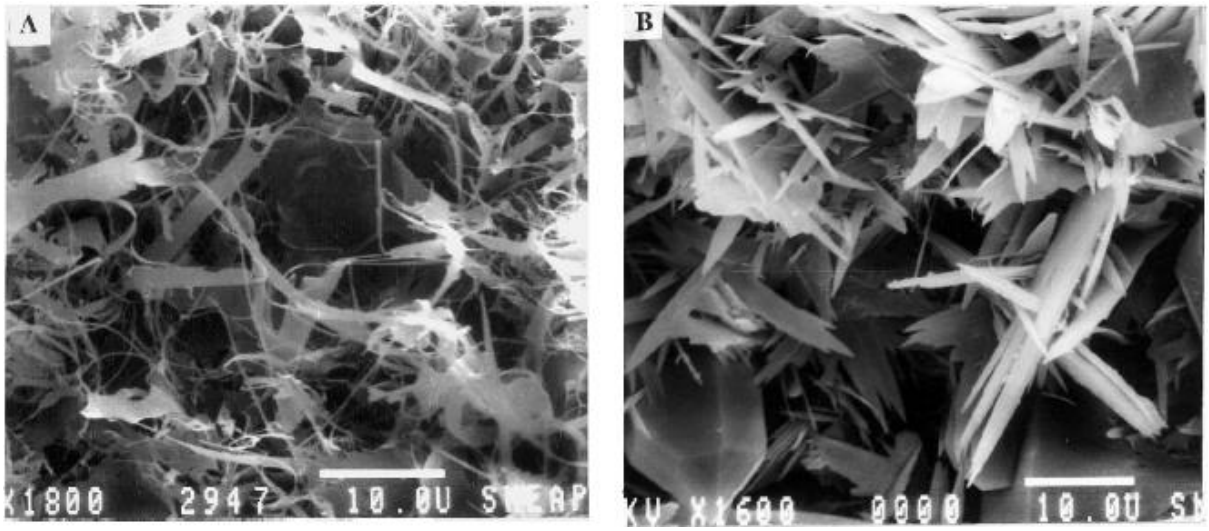

Figure 2.5: Illite crystals at different depths. (A) 3000 m. Elongated, nearly one-dimensional illite crystals. (B) 3500 m. Lath shaped illitic minerals. From (Lanson et al., 2002).

2.4.2 Quartz cementation

Quartz cementation is the most important contributor to porosity loss in deeply buried sandstones (> 2.5 km) (Walderhaug, 1994, Walderhaug, 1996). It is strongly driven by temperature, being present primarily in sandstones heated to 80°C and above. This normally restricts quartz cementation at shallow depths. Such temperatures is normally encountered in deeply buried sandstones, where flow of meteorically derived ground water does not take place (Bjorlykke and Egeberg, 1993). Transportation of dissolved silica is therefore likely to occur as a result of short-distance diffusion (Walderhaug, 1996).

Quartz cement is less abundant in sediments with grain coating clays. Grain coating and microquartz inhibits the formation of quartz cement along the surface of the sediments (Worden and Morad, 2000, Walderhaug, 1996). A more detailed description can be found in the section about porosity preserving mechanisms.

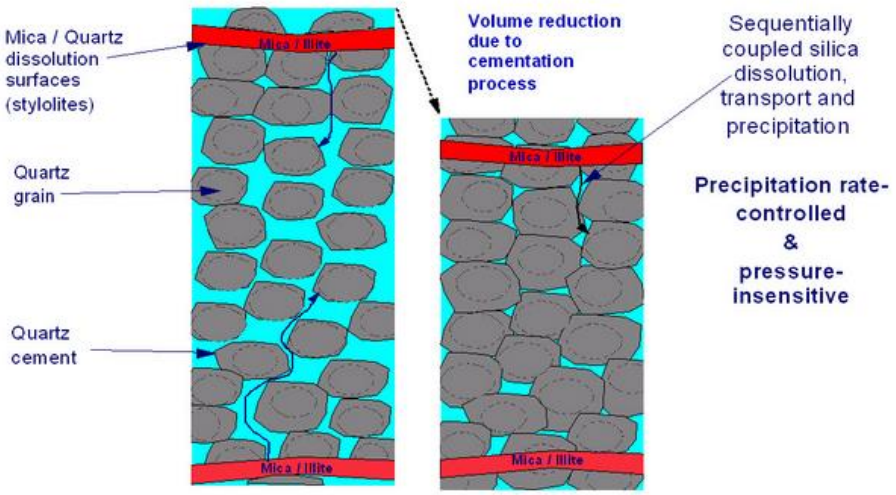

Figure 2.7: Quartz cementation in deeply buried sandstones (Statoil)

A study done by Bjørlykke et al. (1992) shows that quartz cementation in the Brent Group increases significantly at depths below 3 km. However, in some sandstones of the Brent Group located in the Statfjord Field, the amount of quartz cementation is so low that sand production during oil recovery is a complication (Kittilsen, 1987). This can occur in overpressured sandstones. This shows that quartz cement is necessary to strengthen the rock

enough to withhold against effective stress. The strength of the rock relies not solely by the amount of quartz cement, but it is also determined by factors such as sorting, porosity and grain size (Kittilsen, 1987, Walderhaug, 1996). Sandstones with finer grain sizes tend to have more shear strength than coarser grained sandstones (Kittilsen, 1987). Grain size does also, in addition to grain coating, have a considerable effect on quartz cementation as they influence the quartz surface area (Walderhaug, 1994, Walderhaug, 1996). Finer grains will have a larger free surface area per volume of quartz. A mathematical model of quartz cementation, developed by Walderhaug (1996), shows that the porosity difference between fine (0.1 mm) and coarse (0.6 mm) grained sandstones can vary as much as 15% 30 Ma after deposition, depending on mineral assemblage, sorting and initial porosity.

Pre-quartz cementation porosity (IGV) affects the total volume of potential quartz cement and quartz precipitation. More quartz cement would be needed to fill a larger volume of porosity. Therefore, it would take longer for a high porosity sandstone to be completely quartz cemented (Walderhaug, 1996).

Stylolites in sandstones

Stylolites in sandstones occur as seams or as fine structures at grain contacts. They are of particular interest in sandstones because of their effect on porosity and permeability. Additionally, they are believed to be a source of silica in precipitation of quartz cement. The largest stylolites are formed parallel to the bedding, but smaller ones can be observed along cross-laminations or fractures (Milton, 1955). The most accepted theory of stylolite formation is formation by pressure solution (Tada and Siever, 1989). Stress caused by the overburden leads to a grain-to-grain contact dissolution and intergranular volume reduction. Some models include grain interpenetration as a significant source of porosity loss (e.g. Angevine and Turcotte (1983)). However, studies have shown that strongly quartz cemented samples do not show extensive grain interpenetration (e.g Land and Dutton (1978)). Other models, such as Leder and Park (1986) and Walderhaug (1996) either disregard grain interpenetration or finds it negligible, respectively. Dissolved minerals precipitate on free (uncoated) mineral grains as cement, and are expected to precipitate on uncoated grains in close proximity to the stylolite source. The dissolved minerals (i.e. quartz) can be transported by diffusion, but this solution-and-precipitation process reduces porosity and force fluid migration as well. (Angevine and Turcotte, 1983, Bjørlykke and Jahren, 2010).

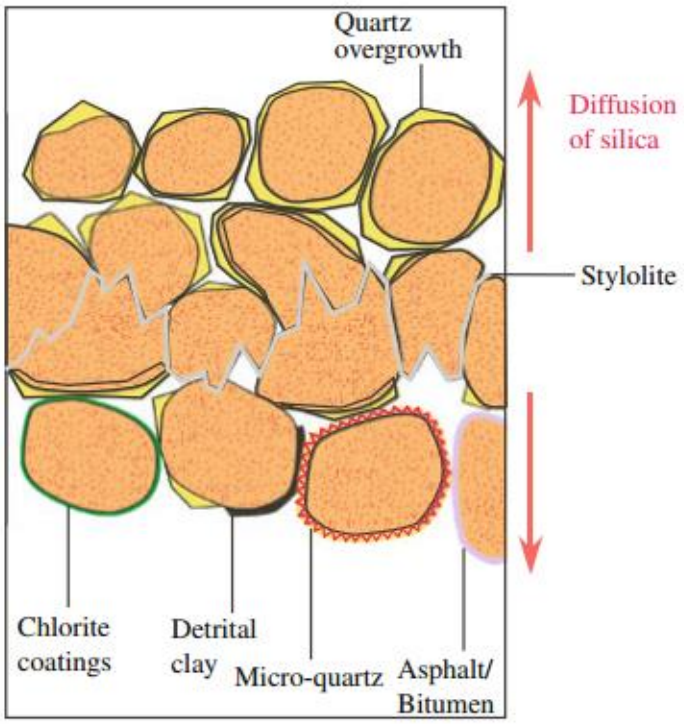

Figure 2.8 : Illustration of stylolites and its surrounding grains. Note that quartz cement doesn't precipitate on coated grains. From Bjørlykke and Jahren (2010).

2.5 Porosity-preserving mechanisms

Most of the diagenetic processes influence the porosity of sandstones. From deposition to cementation we see a general trend of reducing porosity. Mechanical compaction and quartz cementation are shown to be the leading porosity reducing factors. For a reservoir to be profitable it is often important that the reservoir sandstone is also affected by porosity-preserving mechanisms. In literature there are described three main factors that preserve porosity: fluid overpressure, grain coatings and early hydrocarbon emplacement.

2.5.1 Fluid overpressure

If the fluid pressure in a sedimentary rock exceeds the hydrostatic pressure, the effective stress caused by the overburden will be reduced. This is known as overpressure, and can be seen as a porosity preserving factor.

2.5.2 Grain coatings

Grain coating minerals, such as authigenic chlorite and microquartz have been widely accepted as an explanation for preserving high porosity in deeply buried sandstones (Aase et al., 1996). Distribution and occurrence has been reported in several sandstones within the North Sea region (Ehrenberg, 1993). Such coatings can occur both authigenically and allogenically (prior to burial).

2.6 Intergranular volume

Intergranular volume, or IGV, is the degree of porosity loss by mechanical compaction at the onset of chemical compaction. It is an indicator of diagenesis that can give important information when plotted against depth and porosity curves, and cement geochemistry (Szabo and Paxton, 1991). Intergranular volume can be measured by summing intergranular porosity, detrial matrix and cement in thin sections (Szabo and Paxton, 1991). This makes it possible to determine the IGV even in cemented rocks:

Formula 2.4: Calculation of intergranular volume.

$$IGV(\%) = (V_{matrix} + V_{cement}) + V_{intergranular\ porosity}$$

3 Geological Framework

3.1 Introduction

In Early Jurassic the sea level rose (Haq et al., 1987), the climate changed and the basin areas of the North Sea were flooded. A lot of the mainland and the continental shelf were developed into the shape we see today. The climate went from arid to humid, and consequently led to a dramatic change in erosion and deposition. Gravel, sand and mud were now transported from the mainland on to the continental shelf, forming deltas along the coast. (Johannessen and Nøttvedt, 2006).

3.2 Stratigraphic setting

The Brent Group borders to the Viking Group up stratigraphy and to the Dunlin Group down stratigraphy. The Brent Group divides into five formations, defined by Deegan and Scull (1977): Broom (base), Rannoch, Etive, Ness and Tarbert (top). The Broom Formation ranges from shallow to deep-water deposits. A fan delta interpretation is preferred in recent publications (Richards, 1992). The Rannoch and Etive formations are consisting of shoreface and/or foreshore deposits. The Ness Formation consists of deltaic sediments. The Tarbert Formation represents a transgressive unit (Richards, 1992). The lower part of the group (Broom, Rannoch and Etive) consists mainly of very fine to coarse sands, and a small amount of mudstones (Richards, 1992). The coal-bearing Ness Formation, which overlies barrier-bar sediments of the Etive Formation, is a delta succession deposited during progradation of the delta system (Graue et al., 1987).

Table 3.1 Litostratigraphy of the Brent Group as interpreted by Richards (1992).

Formation	Lithology	Depositional env.
Tarbert	Sandstone	Upper shoreface
Ness	Sandstone, siltstone & shale	Lower delta plain
Etive	Sandstone	Upper shoreface
Rannoch	Sandstone	Lower and middle shoreface
Broom	Sandstone	Fan-delta

3.2.1 A short introduction to the lithology of the Rannoch, Etive and Ness formations

Rannoch

The Rannoch Formation is mainly upward coarsening, fine grained, very micaceous and well sorted sandstone. Over much of the East Shetland Basin the Rannoch Formation has a micaceous siltstone unit near the base (Richards, 1992).

Etive

Previous works done on the Etive Formation concludes that it mainly consists of fine to coarse and sometimes pebbly sandstone. The mica content is generally low. Calcite cement is also present in varying degree. It is situated between the underlying, more distal Rannoch Formation and the overlying, more proximal Ness Formation. The Etive formation distinguishes itself from the Rannoch Formation and the Ness Formation in having much lower gamma readings (Vollset and Doré, 1984).

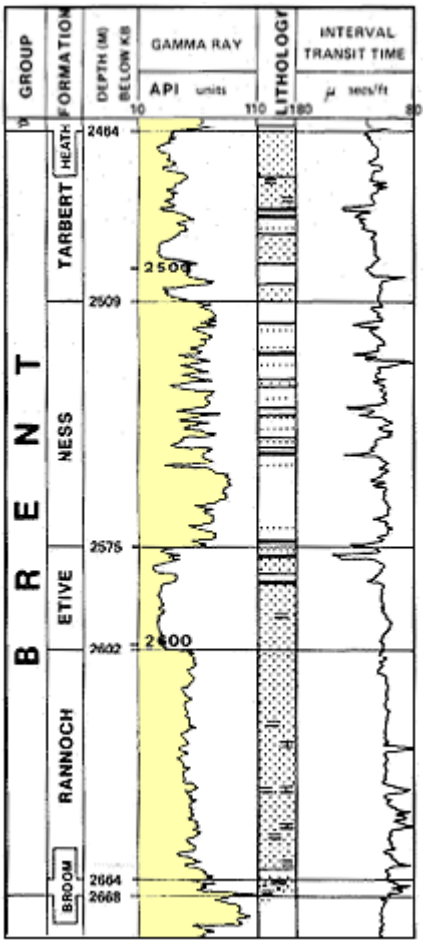

Figure 3.1 Well 33/9-1 showing the gamma ray readings (pale yellow) in each of the Brent formations (Vollset and Doré, 1984).

Ness

The Ness Formation is the youngest and most lithologically variable unit of the three. It consists of an association of coals, shales, siltstones and very fine to medium grained sandstones. The shales are silty and often pyritic. The varying lithology produces an irregular gamma ray and sonic response (Vollset and Doré, 1984).

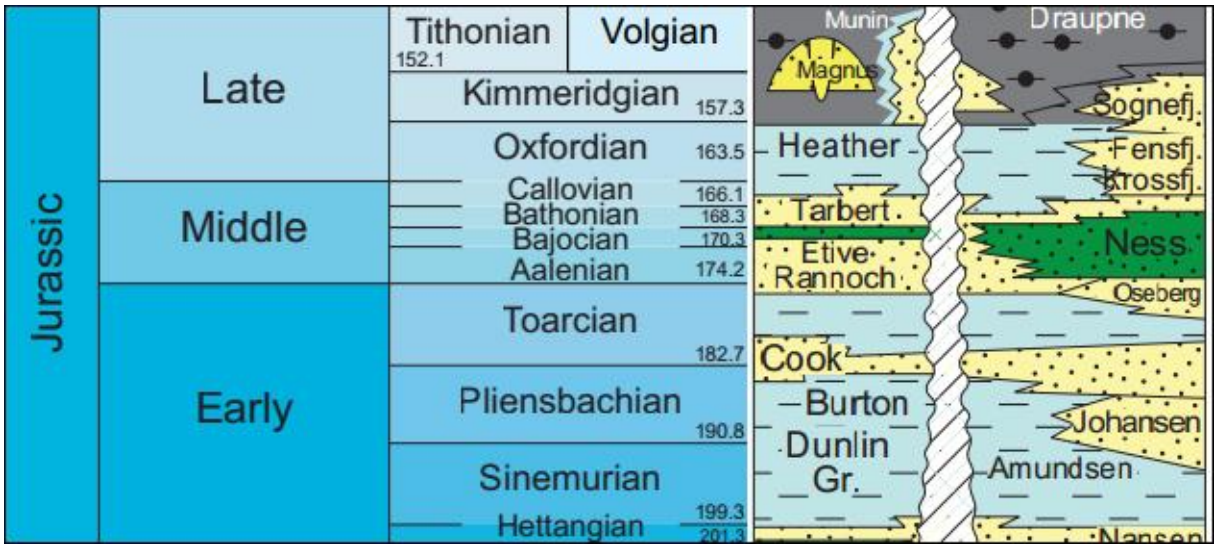

Figure 3.2 Stratigraphic chart of the Jurassic period from the Northern Viking Graben (Norlex, 2014)

3.2.2 Sequence stratigraphic framework of the Middle Jurassic

The shoreline moved basinward and landward numerous times during Early and Middle Jurassic. Periods of little subsidence combined with a high sediment influx moved the shoreline basinward. Periods of higher subsidence led to a rise in sea level and moved the shoreline more landward (Johannessen and Nøttvedt, 2006).

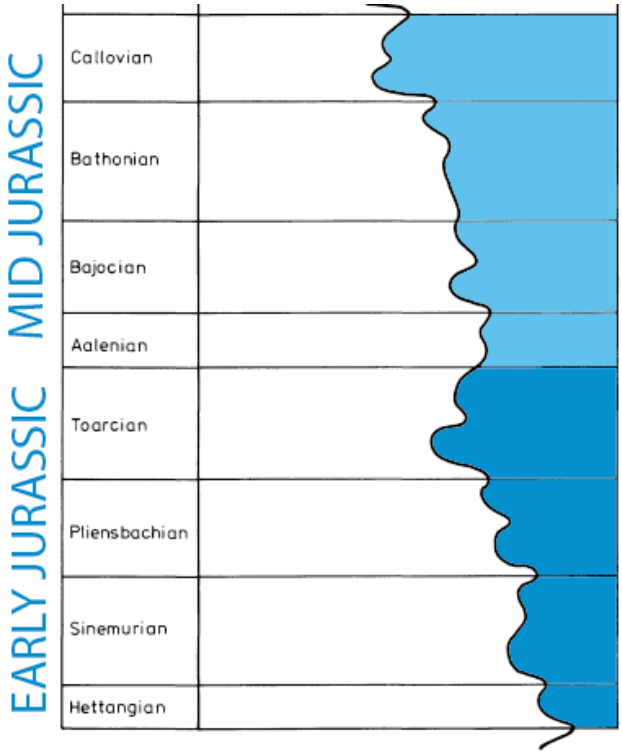

Figure 3.3 Proposed sea level curve for the Jurassic, modified after Hallam (1988).

Earlier interpretations suggest that the sea level was quite stable, or slightly rising, during Middle Jurassic (Aalenian-Bajocian) when the Etive Formation was deposited (Olsen and Steel, 2000). The evidence for this scenario include gradual upward facies change between the formations and of time lines passing through the Etive into the Rannoch Formation (Olsen and Steel, 2000). More recent publications argue that there are indicators suggesting a more irregular shoreline progradation at certain times, and for falls of sea level and forced regression (Olsen and Steel, 2000). The evidence is focused around the presence of incised valleys (Jennette and Riley, 1996) and deep erosion/subaerial exposure surfaces (Reynolds, 1995) from the Etive-Ness boundary and the more distal Etive-Rannoch reaches of the Brent system. Olsen and Steel (2000) argue in their paper that both scenarios negate the other, and conclude that the possibility for both happening in a time span of 4 Ma is unlikely.

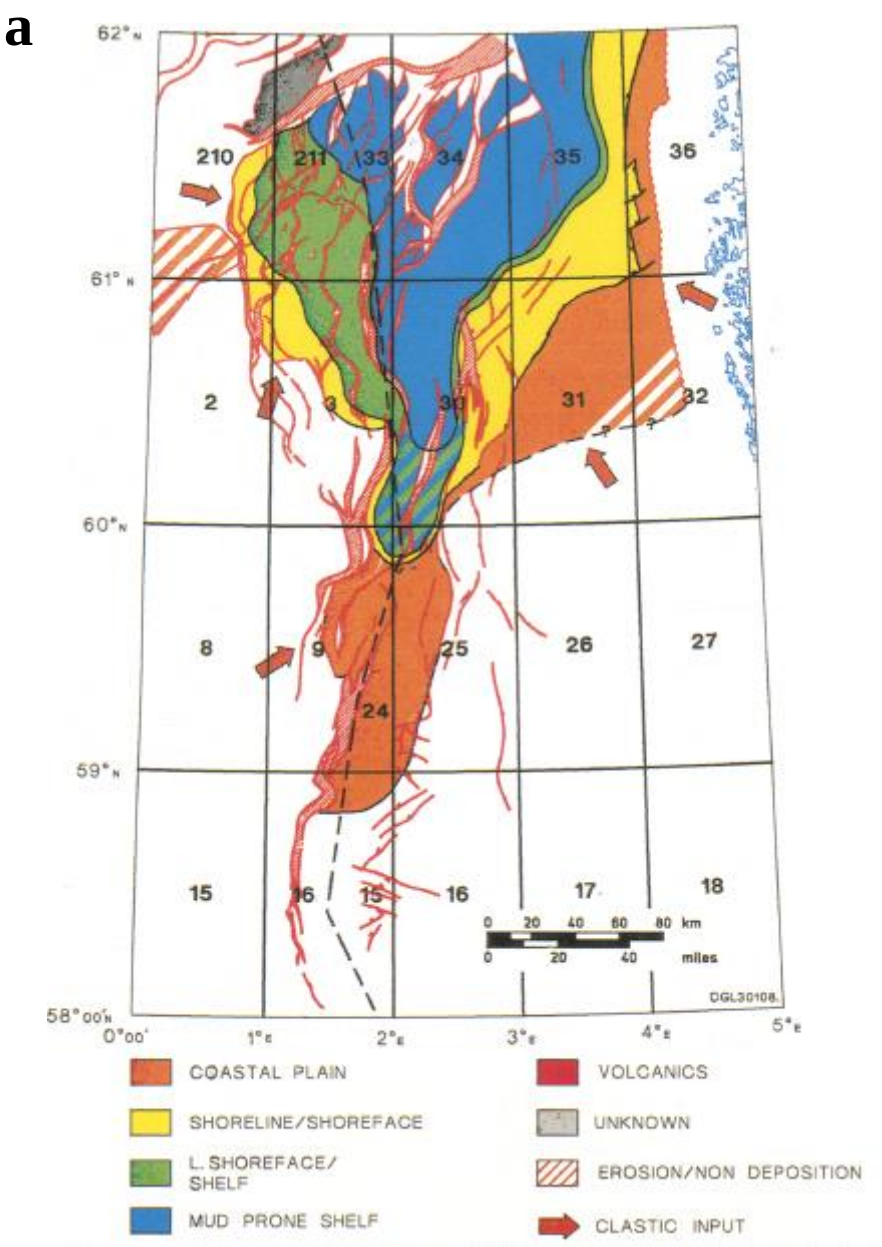

Figure 3.4: a) Aalenian depositional environments, **b)** Early-Late Bajocan depositional environments. From Mitchener et al. (1992).

b

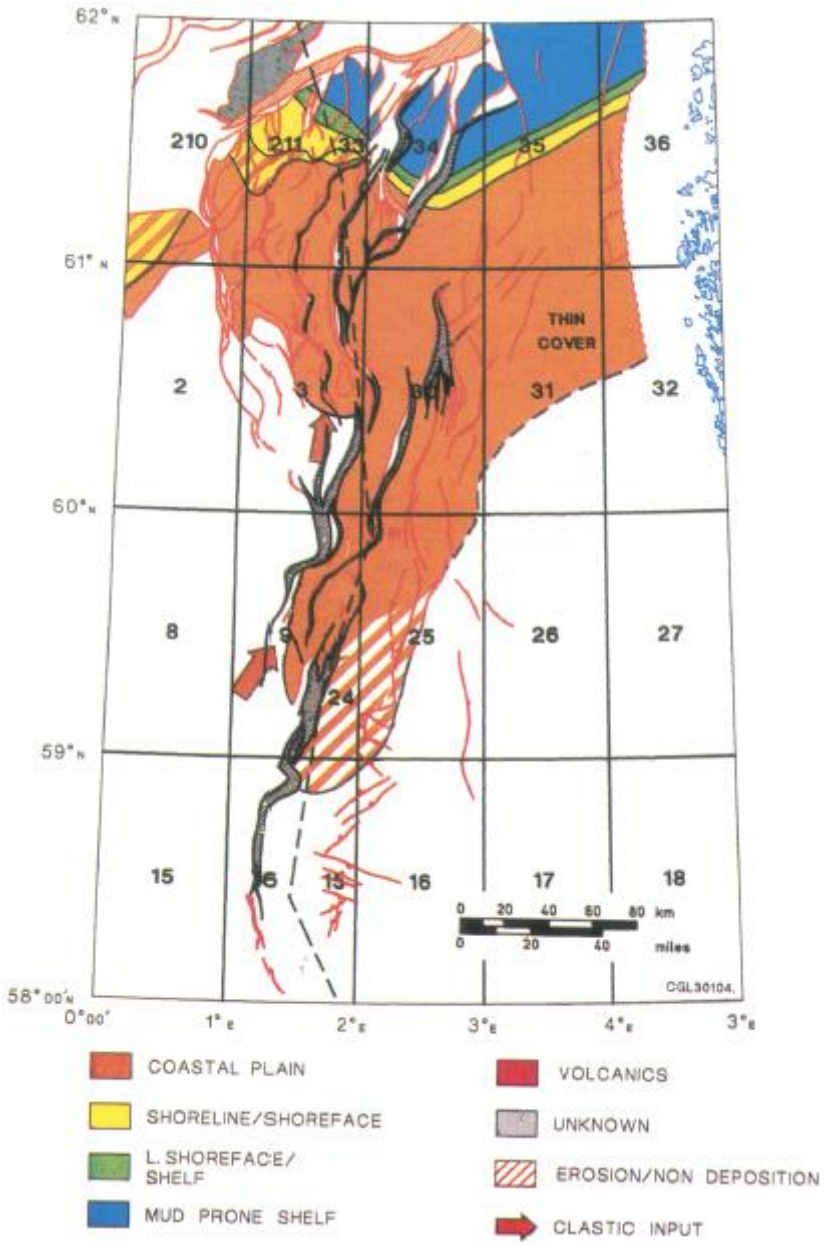
62°N
61°N
60°N
59°N
58°00'N
0°00'
1°E
2°E
3°E
4°E
5°E
210
211
33
34
35
36
THIN COVER
2
3
31
32
8
9
25
26
27
24
15
16
17
18
0 20 40 60 80 km
0 20 40 miles
CGL30104.
COASTAL PLAIN
SHORELINE/SHOREFACE
L. SHOREFACE/ SHELF
MUD PRONE SHELF
VOLCANICS
UNKNOWN
EROSION/NON DEPOSITION
CLASTIC INPUT

3.3 Structural setting of the North Sea

The North Sea Rift is a N-S oriented, approximately 150-200 km wide zone separating the Horda Platform in the east from the East Shetland Platform in the west (Fjeldskaar et al., 2004). During Permo-Triassic and late Jurassic two main rifting episodes separated by 125 Ma is recognized in the Northern Viking Graben (Yielding et al., 1992). Each rifting episode was followed by a period of thermal cooling, characterized by regional subsidence (Yielding et al., 1992, Christiansson et al., 2000). Because of these episodes we see structures such as large rotated fault blocks with sedimentary basins in asymmetric half-grabens associated with extension and thinning of the crust within the area (Fjeldskaar et al., 2004).

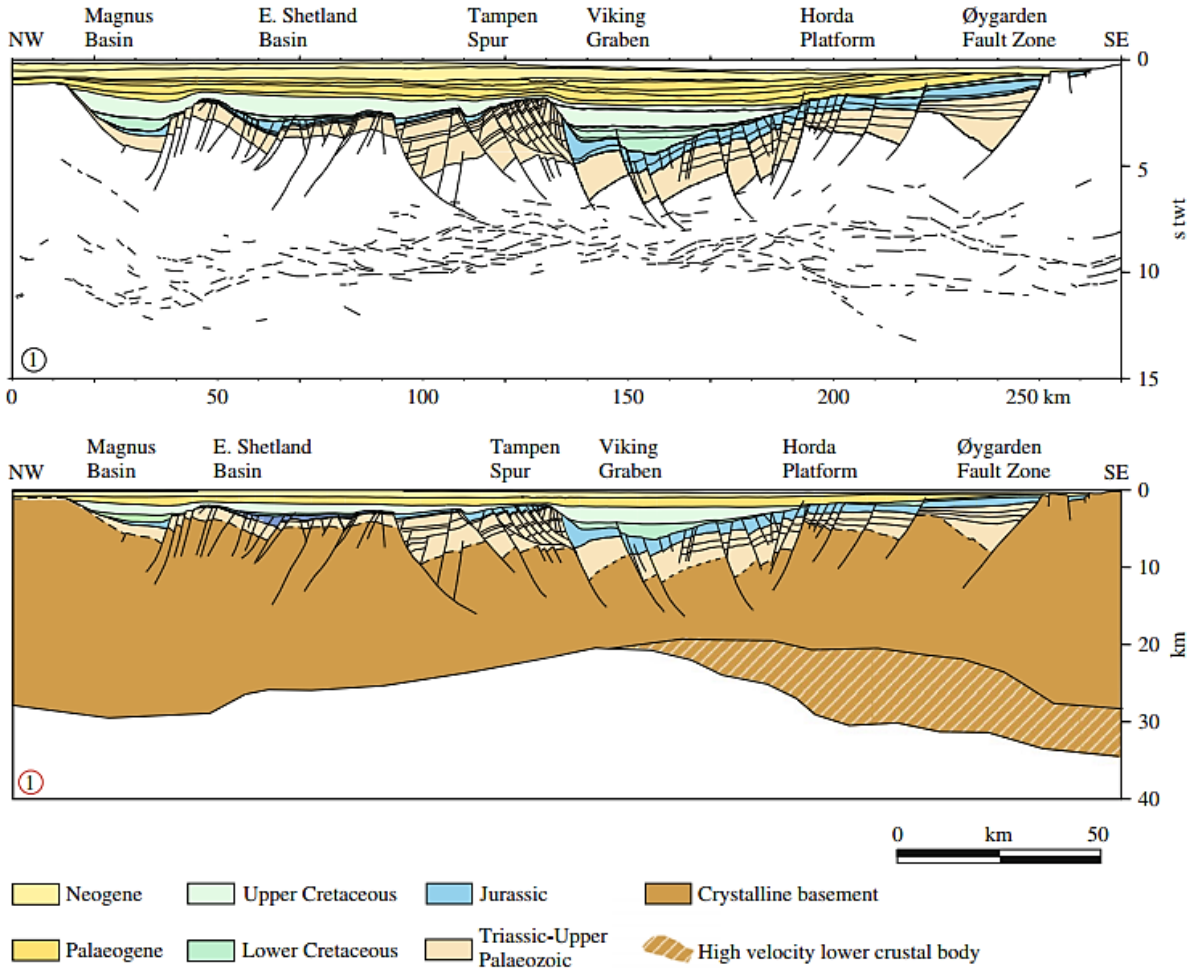

Figure 3.5 Interpreted regional deep seismic line and crustal transect across the northern North Sea (Faleide et al., 2010) (modified from Christiansson et al. (2000)).

The Permo-Triassic event was the first of the two rifting episodes, and was followed by a period of post-rift thermal cooling during Early-Mid Triassic (Fjeldskaar et al., 2004). Later, Extension in the Jurassic resulted in large tilted fault blocks which today serve as hydrocarbon traps (Fjeldskaar et al., 2004), and is known as the second rift stage. This affected the North Sea basin from late Middle Jurassic to earliest Cretaceous (Fjeldskaar et al., 2004). Faults generated during the Jurassic extension seem to be rooted in older structures, indicating that the old basement faults may have been reactivated during the two rifting episodes (Fjeldskaar et al., 2004).

3.3.1 Structural setting of the Brent Group

The evolution of the Viking Graben serves as the essential control on the deposition of the Brent Group, and on the mechanisms of hydrocarbon trapping. The Brent Group was deposited before the renewed rifting in late Jurassic, meaning the main structural control of deposition was the thermal subsidence after the early Triassic stretching. It was this subsidence that made the trough, in which the Brent delta was able to prograde into. During late Jurassic there was a second rifting episode, which caused the fault blocks to move, rotate and essentially create the fault traps we see today. The late Jurassic extension resulted in wedge-shaped sediment packages that infill the rotated fault blocks (Yielding et al., 1992).

4 Methods and data

4.1 Petrographic analysis

4.1.1 Thin section analysis

A Nikon polarizing petrographic microscope was used to analyse 2D thin sections from different wells at different depths of the Rannoch, Etive and Ness formations. These were studied in different magnifications, depending on grain size. Methods and/or properties used to identify minerals include: pleochroism, relief, Becke line, interference colours and birefringence (see Nesse (2004)). The reason for doing a thin section analysis is mainly to establish information about mineral assemblage, texture, cementation and porosity.

A total of 55 thin sections were analysed (18 from the Ness Formation, 20 from the Etive Formation and 17 from the Rannoch Formation), from 14 different wells. Some of the wells are included in fields, such as the Statfjord Field, and some are not.

Each thin section was point counted 300 times, and the results recorded in a spread sheet.

Table 1: Wells used in thin section analysis by formation.

Ness Formation	Etive Formation	Rannoch Formation
34/10-3	34/10-3	34/10-4
35/9-1	34/7-12	34/7-12
30/6-10	35/11-1	35/11-1
30/3-3	30/6-10	30/3-2R
34/10-23	33/9-3	33/6-1
	34/10-17	34/10-23
	34/10-23	

Legend
Gullfaks
Tordis
Oseberg
Veslefrikk
Statfjord
Valemon
No field

4.1.2 SEM analysis

The scanning electron microscope (SEM) is a microscope that uses electrons instead of light to form an image, allowing a much higher resolution and depth of field. It also has the trait of identifying elements present in a single point and/or in a larger quadrant. This is advantageous when identifying small (µm) objects. A JEOL JSM- 6460LV Scanning Electron Microscope (SEM) with a LINK INCA Energy 300 (EDS) system from Oxford Instrument were utilized using BSE (backscattered electrons) on carbon coated thin sections. In this study SEM was mainly used to identify and confirm minerals in the thin sections, which were difficult to determine using the optical microscope. It was also used to study the distribution of clays in pore-space.

No cathodoluminescence detector (CL) was available during the SEM analysis.

4.1.3 Grain size and sorting analysis

A petrographic microscope with an attached camera was used to determine the grain sizes of the different thin sections. A 3 MP camera was linked to a computer using ScopeView 3.0.

50 grains of each thin section was measured along their longest axis. The data was later imported to GRADISTAT © Simon Blott, a grain size distribution and statistics software for sediments.

4.1.4 Uncertainties regarding petrographic analysis

The main concern regarding a petrographic analysis is inexperience with mineral identification and point counting. When using an optical microscope there is a chance of misinterpreting optical properties and thereby polluting the results with wrong mineral data. An example is the thickness of the thin sections. Some thin sections were thicker than the standard 3 µm, which would influence the interference colours. Another issue is that some of the thin sections used were old, and prepared with other standards and equipment than used today. Some of the thin sections showed signs of grain loss, creating large areas of apparent porosity. This may lead to inaccurate porosity measurements.

When doing a grain size analysis it is important that the measured grains are selected as randomly as possible. It is impossible to get an absolutely random set of grains when selected manually. This can affect the grain size and sorting results.

The cathodoluminescence detector was unfortunately out of order. Therefore, the volume of quartz cement was calculated by point counting only and thus subject to uncertainty.

5 Petrographic analysis

5.1 Introduction

The mineral compositions of the all three formations were apprehended through thin section analysis. SEM analysis was performed to classify possible grain coatings, to identify authigenic and detrial mineral grains, and to get a second estimate of mineral content and distribution through area measurements. The CL was not functioning at the time, ruling out the possibility to estimate the quartz cement volume.

No core samples of the wells used in this paper were available for study. This excludes the possibility for an XRD analysis, as well as limiting the SEM analysis to thin sections only.

Results from the point counting, grain size analysis, sorting and the SEM analysis will be presentet in this chapter.

5.2 Composition and texture of the Ness Formation

Based on the point counting results (table 5.1) the average Ness Formation sandstone is classified as $Q_{92}F_6R_2$, meaning 92% quartz, 6% feldspar and 2% lithic rock fragments. Therefore, the average Ness sands are classified as quartzarenite (fig. 5.1). It should be noted that the detrial mineral composition varies with depth.

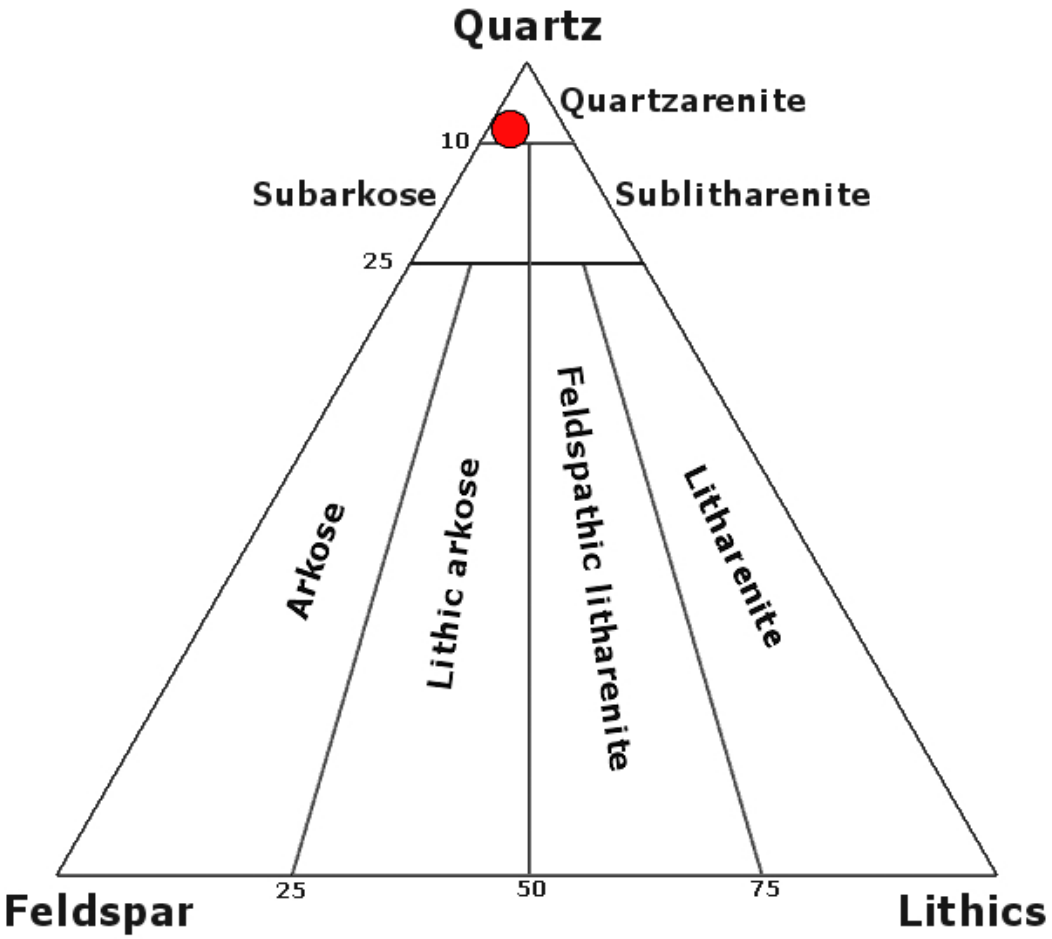

Figure 5.1: Average QFR of sandstones from the Ness Formation samples classified in Folk's classification of sandstones (Folk, 1968).

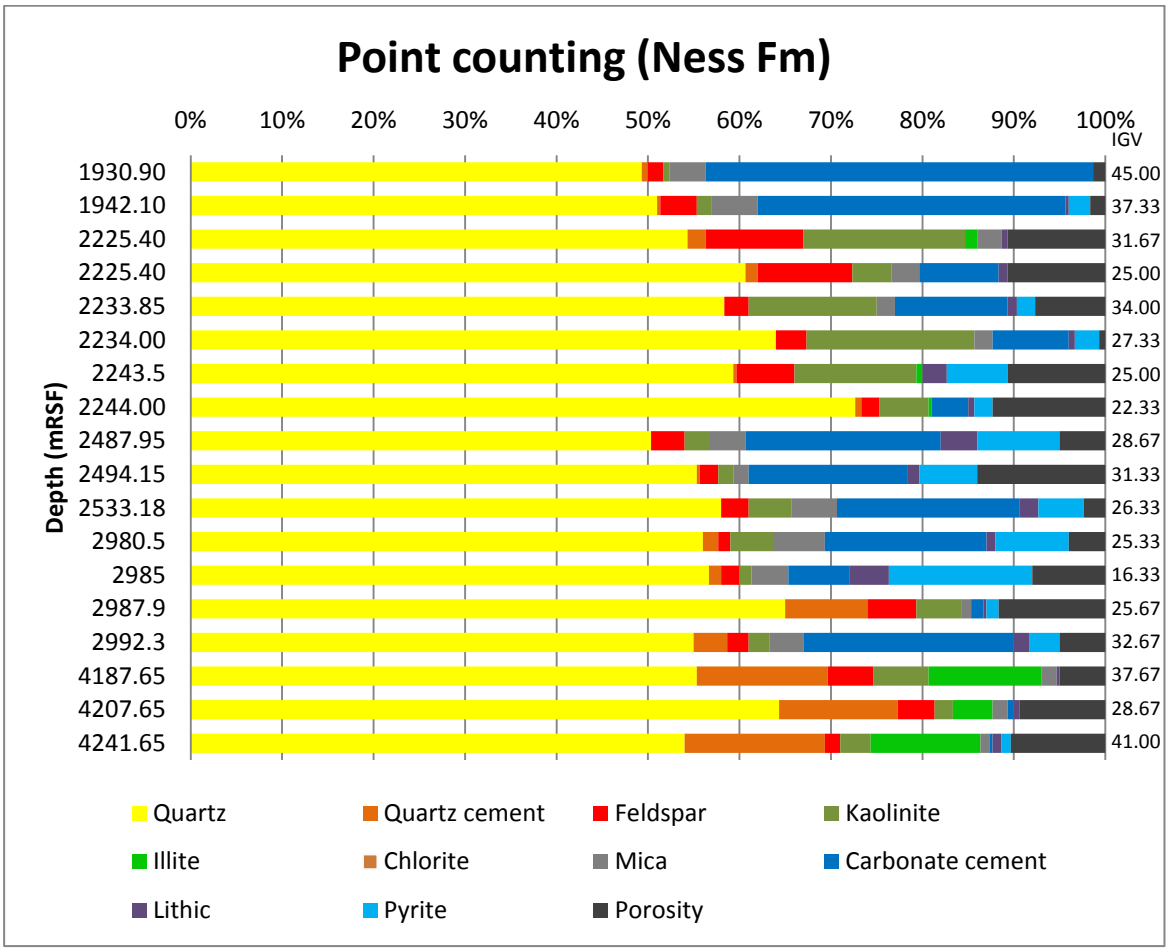

Figure 5.2: Point counting results from the Ness Formation.

5.2.1 Framework mineralogy

Quartz

Quartz grains dominate the framework with a 92% average of the framework grains and a 58 % average of the total mineral composition, including the matrix. The grains are colorless and mainly angular to subangular in shape.

K-feldspar ($KAlSi_3O_8$) and albite ($NaAlSi_3O_8$)

The amount of feldspar grains varies between 1% and 11% throughout the Ness Formation (including the matrix). The average feldspar content is 4% including the matrix, and 7% when considering the framework grains only. Both K-feldspar and albite were observed in the Ness Formation. K-feldspar is the dominant feldspar in the shallower buried samples (1930 m to 2500 m). It is easily recognized by its characteristic twinning structure. The K-feldspar grains

normally dissolve with depth, creating secondary porosity. Albite occurs as a result of albitization of plagioclase grains, and is not as easily dissolved.

Residual framework and detrial clays

Mica was found in 16 of 18 samples with an average of 2.5%. Chlorite was not observed using the petrographic microscope.

5.2.2 Cements

Quartz

The amount of quartz cement varies throughout the formation from less than 1% to 15.3%. The highest contents of quartz cement are found in the deepest buried samples in well 34/10-23 (4187.65 m, 4207.65 m and 4241.65 m), with an average of 14%. These numbers must be considered with the fact that they derive solely from point counting in a petrographic microscope, with no CL available. The process of discriminating cement from quartz grains can be a difficult task if the dust rims aren't obvious, and is therefore subject to uncertainty.

Carbonate

6 samples had no observable carbonate cement, while the rest had carbonate cementation varying from 4% to 42%. The amount of cement in each sample was irregular with respect to depth, although the highest amounts were observed in the shallowest buried samples (<2km). The average for the whole formation was 11.5%.

Kaolinite

Kaolinite was found in all thin sections, varying from less than 1% to 18%. The highest amounts were found in depths between 2.2 km – 2.9 km, with an average of 9%. The amount of kaolinite varied greatly from well to well. Well 35/9-1 had a considerably higher amount than the others, with an average of 12.7% kaolinite. The kaolinite was primarily pore filling, often seen in secondary pores as a result of dissolved K-feldspar.

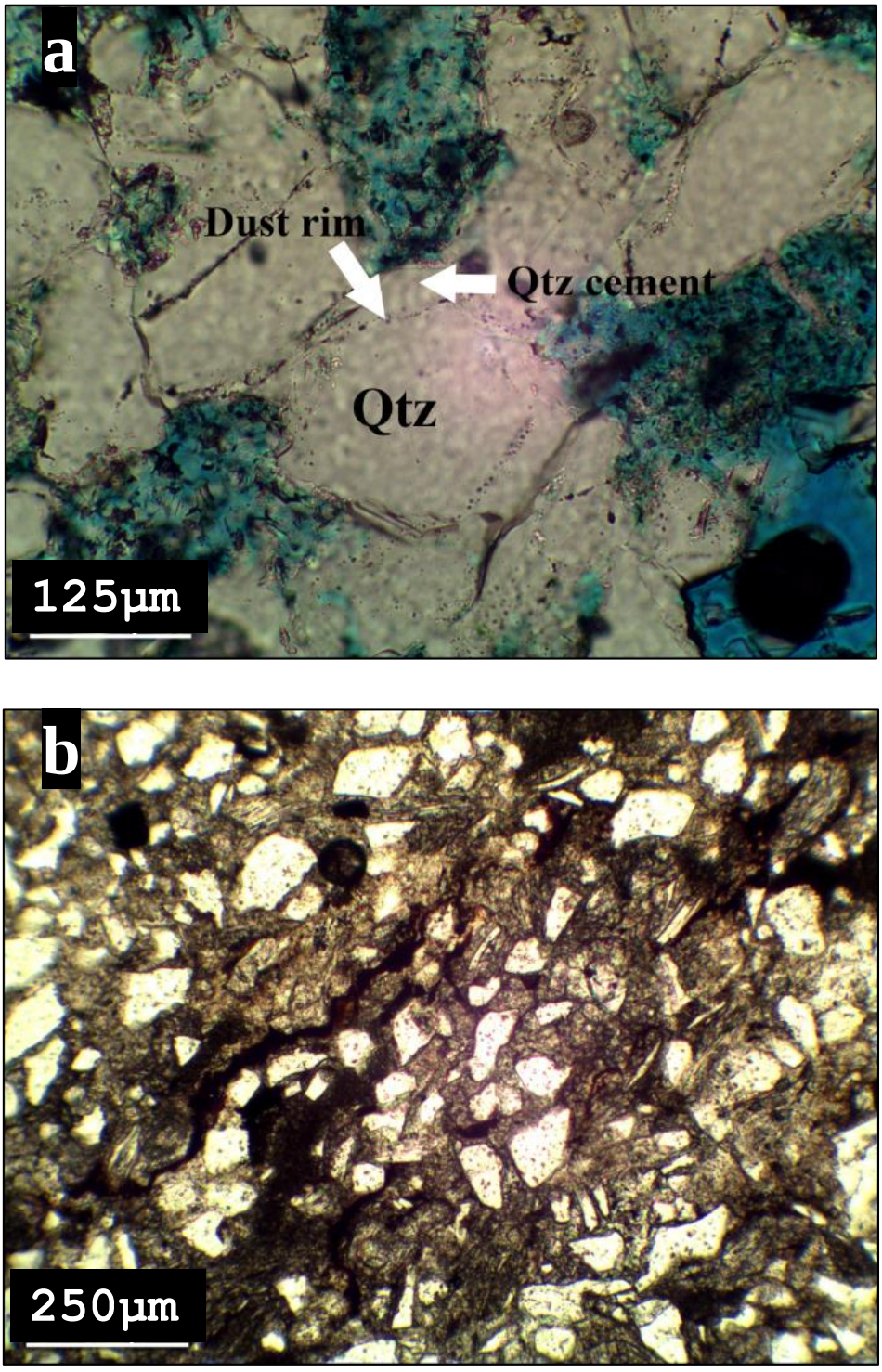

Figure 5.3: Ness Formation. a) Quartz cement at 4187.65 m from well 34/10-23, b) Heavily carbonate cemented sandstone at 1930.9 m from well 34/10-3.

Illite

Authigenic illite was observed in all 3 samples buried below 4 km. The amount in each of those samples varied from 4% to 12%, with an average of 9.5%.

Pyrite

Pyrite is observed in every sample except 5. Samples from well 30/6-10 and 33/3-9 had a higher amount of pyrite, compared to the others. These were present as individual crystals, clusters or veins. The total average was 3.5%. The average content of pyrite in well 30/6-10 and 33/3-9 was 7%.

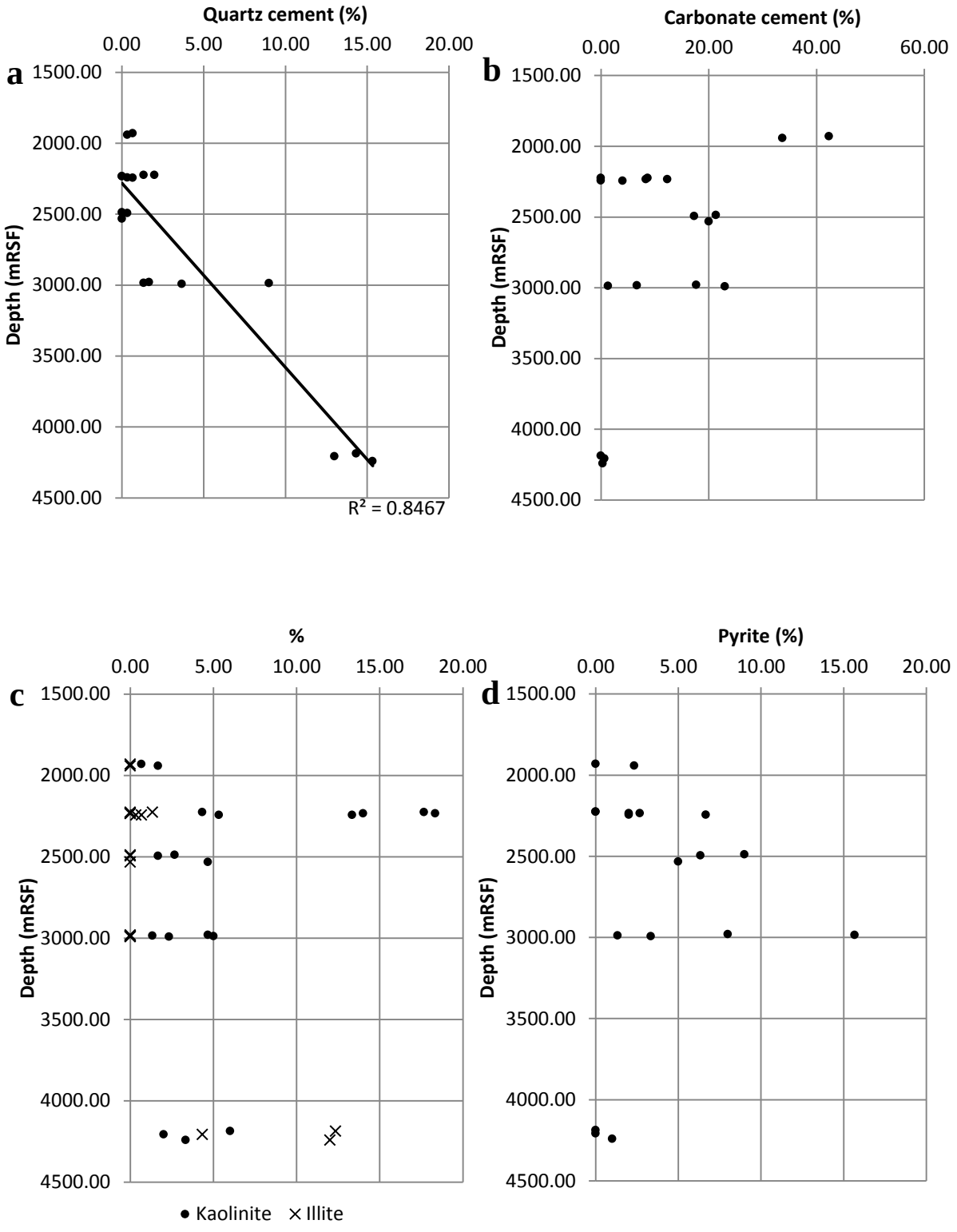

Figure 5.4: Ness Formation a) Quartz cement versus depth, b) carbonate cement versus depth, c) kaolinite and illite versus depth and d) pyrite versus depth.

Table 5.1: The point counting results for the Ness Formation. The results are given in percentage unless specified.

Well	Depth (mRSF)	Framework				Cement						Porosity	IGV	Sorting (log φ)	Avg. grain size (µm)
		Quartz	Feldspar	Mica	Lithic	Kaolinite	Illite	Chlorite	Quartz cement	Carbonate cement	Pyrite				
34/10-3	1930.90	49.33	1.67	4.00	0.00	0.67	0.00	0.00	0.67	42.33	0.00	1.33	45.00	0.614	90
34/10-3	1942.10	51.00	4.00	5.00	0.33	1.67	0.00	0.00	0.33	33.67	2.33	1.67	39.67	0.559	130
35/9-1	2225.40	54.33	10.67	2.67	0.67	17.67	1.33	0.00	2.00	0.00	0.00	10.67	31.67	0.684	499
35/9-1 (2)	2225.40	60.67	10.33	3.00	1.00	4.33	0.00	0.00	1.33	8.67	0.00	10.67	25.00	0.646	467
35/9-1	2233.85	58.33	2.67	2.00	1.00	14.00	0.00	0.00	0.00	12.33	2.00	7.67	36.00	0.762	308
35/9-1	2234.00	64.00	3.33	2.00	0.67	18.33	0.00	0.00	0.00	8.33	2.67	0.67	30.00	0.924	404
35/9-1	2243.5	59.33	6.33	0.00	2.67	13.33	0.67	0.00	0.33	0.00	6.67	10.67	31.67	0.964	446
35/9-1	2244.00	72.67	2.00	0.00	0.67	5.33	0.33	0.00	0.67	4.00	2.00	12.33	24.33	0.844	636
30\6-10	2487.95	50.33	3.67	4.00	4.00	2.67	0.00	0.00	0.00	21.33	9.00	5.00	38.00	0.445	66
30\6-10	2494.15	55.33	2.00	1.67	1.33	1.67	0.00	0.00	0.33	17.33	6.33	14.00	39.67	0.658	114
30\6-10	2533.18	58.00	3.00	5.00	2.00	4.67	0.00	0.00	0.00	20.00	5.00	2.33	32.00	0.428	71
30\3-3	2980.5	56.00	1.33	5.67	1.00	4.67	0.00	0.00	1.67	17.67	8.00	4.00	36.00	0.545	77
30\3-3	2985	56.67	2.00	4.00	4.33	1.33	0.00	0.00	1.33	6.67	15.67	8.00	33.00	0.469	128
30\3-3	2987.9	65.00	5.33	1.00	0.33	5.00	0.00	0.00	9.00	1.33	1.33	11.67	27.00	0.445	244
30\3-3	2992.3	55.00	2.33	3.67	1.67	2.33	0.00	0.00	3.67	23.00	3.33	5.00	37.33	0.777	97
34/10-23	4187.65	55.33	5.00	1.67	0.33	6.00	12.33	0.00	14.33	0.00	0.00	5.00	37.67	0.468	198
34/10-23	4207.65	64.33	4.00	1.67	0.67	2.00	4.33	0.00	13.00	0.67	0.00	9.33	29.33	0.596	280
34/10-23	4241.65	54.00	1.67	1.00	1.00	3.33	12.00	0.00	15.33	0.33	1.00	10.33	42.00	0.711	161
Average		**57.76**	**3.96**	**2.67**	**1.31**	**6.06**	**1.72**	**0.00**	**3.56**	**12.09**	**3.63**	**7.24**	**34.19**	**0.64**	**245.33**

5.2.3 Porosity

Porosity varies greatly throughout the formation from less than 1% to 14%, with an average of 7%. The porosity is lower in samples dominated by cements.

5.2.4 Intergranular volume and textural parameters

The average IGV is 34.2% when including all samples. One sample (well 34/10-3 1930.9 m) showed an abnormally high IGV of 45%.

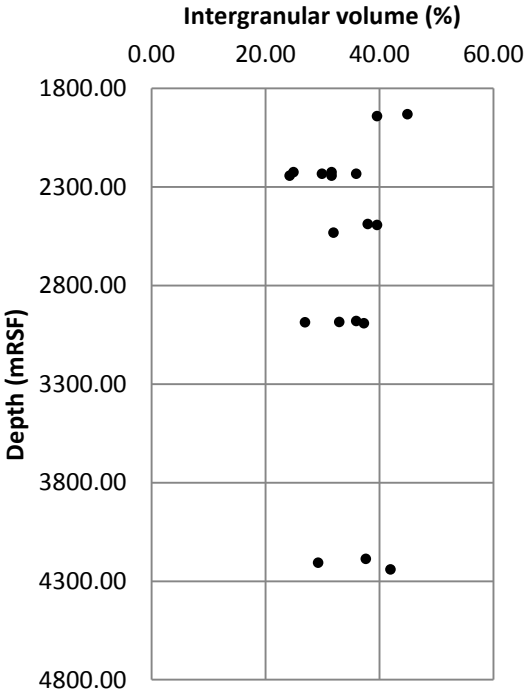

Figure 5.5: Intergranular volume versus depth in the Ness Formation.

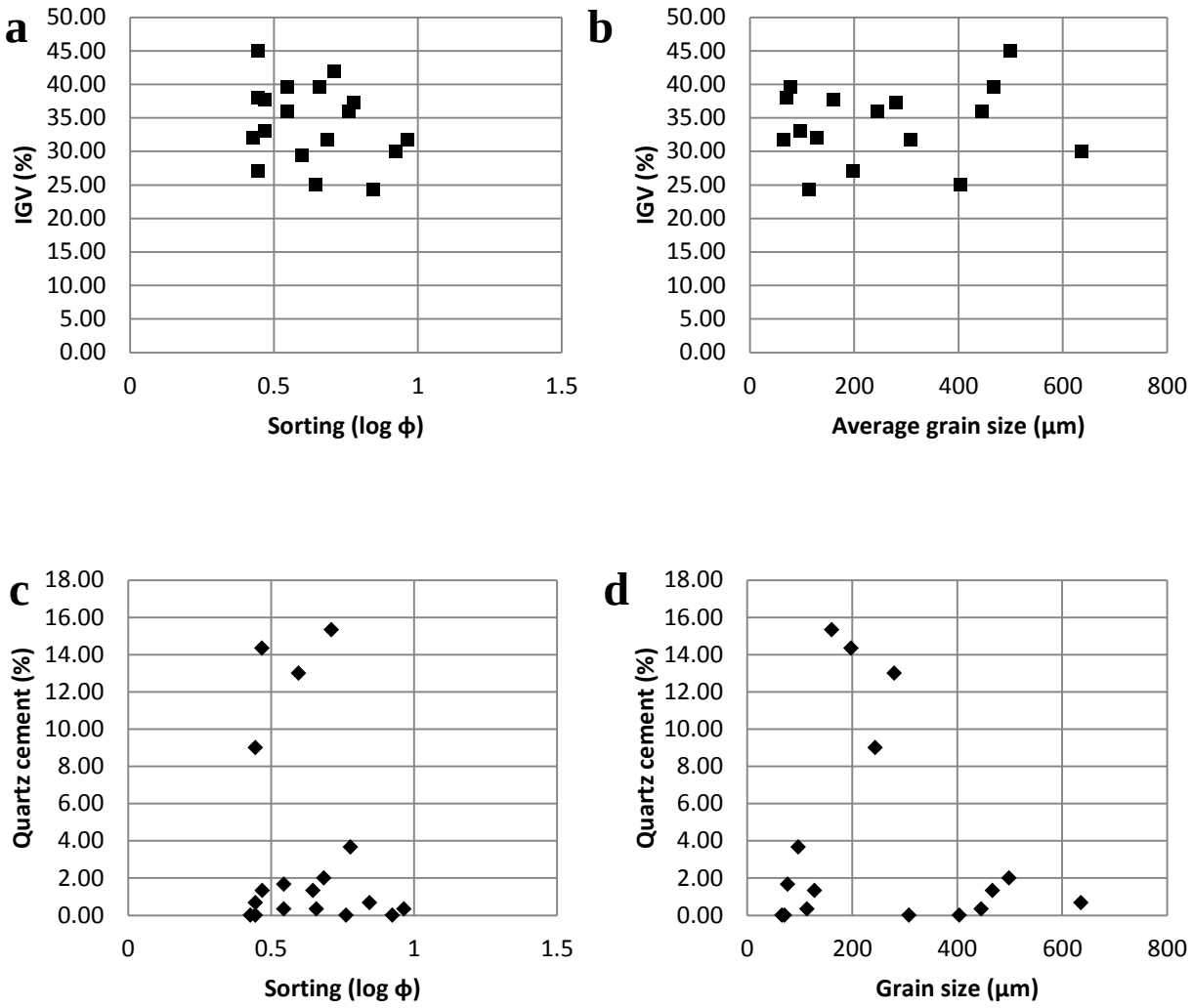

Figure 4.x: Ness Formation. a) IGV versus sorting (logarithmic folk method), b) IGV versus average grain size, c) quartz cement versus sorting and d) quartz cement versus average grain size.

5.3 Composition and texture of the Rannoch Formation

The result from the point counting classifies the Rannoch sandstone as $Q_{83}F_{14}R_3$, sandstone consisting of 83% quartz, 14% feldspar and 3% lithic fragments. Thus the average Rannoch sand is subarkose.

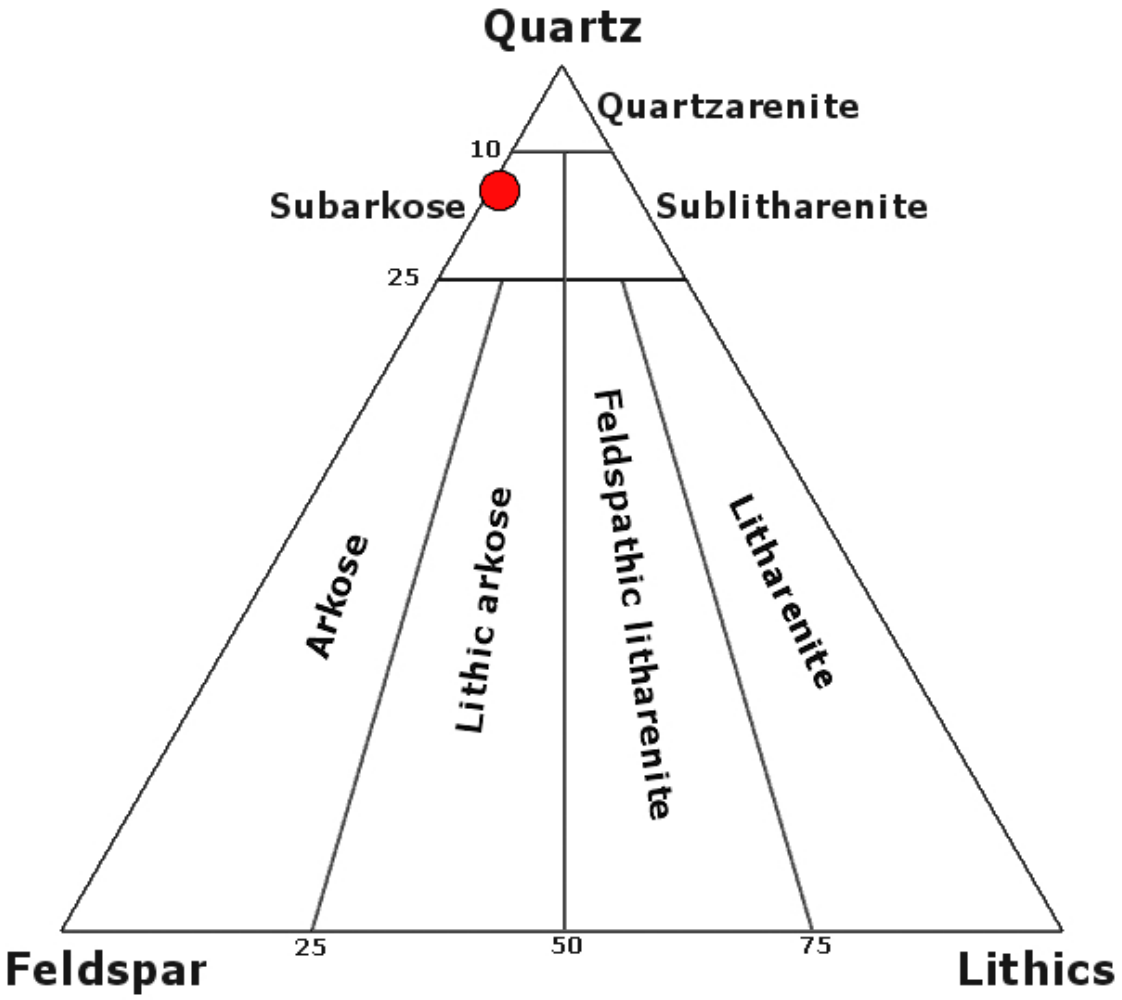

Figure 5.6: Average QFR of sandstones from the Rannoch Formation samples classified in Folk's classification of sandstones (Folk, 1968).

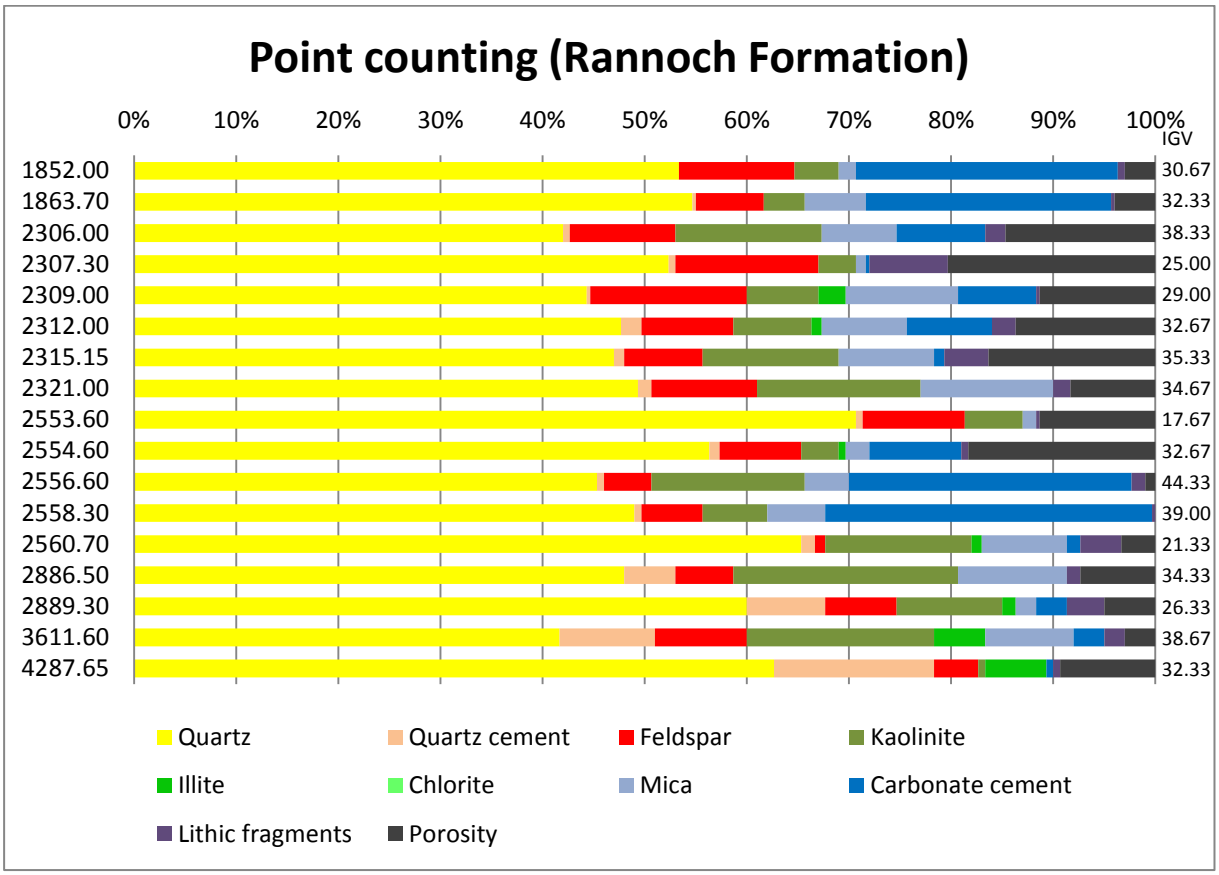

Figure 5.7: Point counting results from the Rannoch Formation.

5.3.1 Framework mineralogy

Quartz

Quartz grains dominate the framework with an 83% average of the framework grains and a 52% average of the total mineral composition, including the matrix. The grains are colourless and mainly angular to subangular in shape.

K-feldspar ($KAlSi_3O_8$) and albite ($NaAlSi_3O_8$)

The Rannoch Formation is dominated by two types of feldspar; K-feldspar and albite. Their formation and behavior has been discussed in previous chapters. The feldspar content in each of the samples ranges from 1.4% to 26% of the framework composition, and 1% to 15% of the total mineral composition. The average feldspar content is 8%. The amount feldspar is noticeably higher in samples buried from 1.8 km to 2.5 km than >2.5 km. The average feldspar content in samples buried <2.5 km is 11%, and 6% in samples buried >2.5 km.

Residual framework and detrial clays

Mica was found in 16 of 17 samples. The average mica content for the Rannoch Formation is 6%. Chlorite was not observed using a petrographic microscope.

5.3.2 Cements

Quartz

The average quartz cement content for the whole formation is 2.8%, with sample amounts varying from less than 1% to 15.6%. The highest amount is found in the deepest buried sample from well 34/10-23 (4287.65 m), with a quartz cement content of 15.6%. With no CL available, these numbers are subjects to uncertainty.

Carbonate

Carbonate cements were observed in 14 of 17 of the samples, with an average of 9%. The amount ranges from 0% to 32%. The degree of cementation was noticeably varying from well to well. Well 34/10-4 and 35/11-1 had the highest amount of cement, with averages of 28.8% and 14%.

Kaolinite

Kaolinite was found in all thin sections ranging from less than 1% to 22%. The average for the Rannoch Formation was 9.8%. The kaolinite amount was highest in samples buried from 2.3 km to 3.6 km, with an average of 11.3%. Well 30/3-2R had the largest kaolinite content with an average of 16%. The kaolinite was primarily pore filling, precipitated as a result of dissolved mica or K-feldspar in secondary pores.

Illite

Illite was present in 7 of 17 samples. Authigenic illite was observed in samples buried deeper than 3.6 km, with an average amount of 5.5%. Some of the shallower buried samples showed detrial illite crystals either in or around micas.

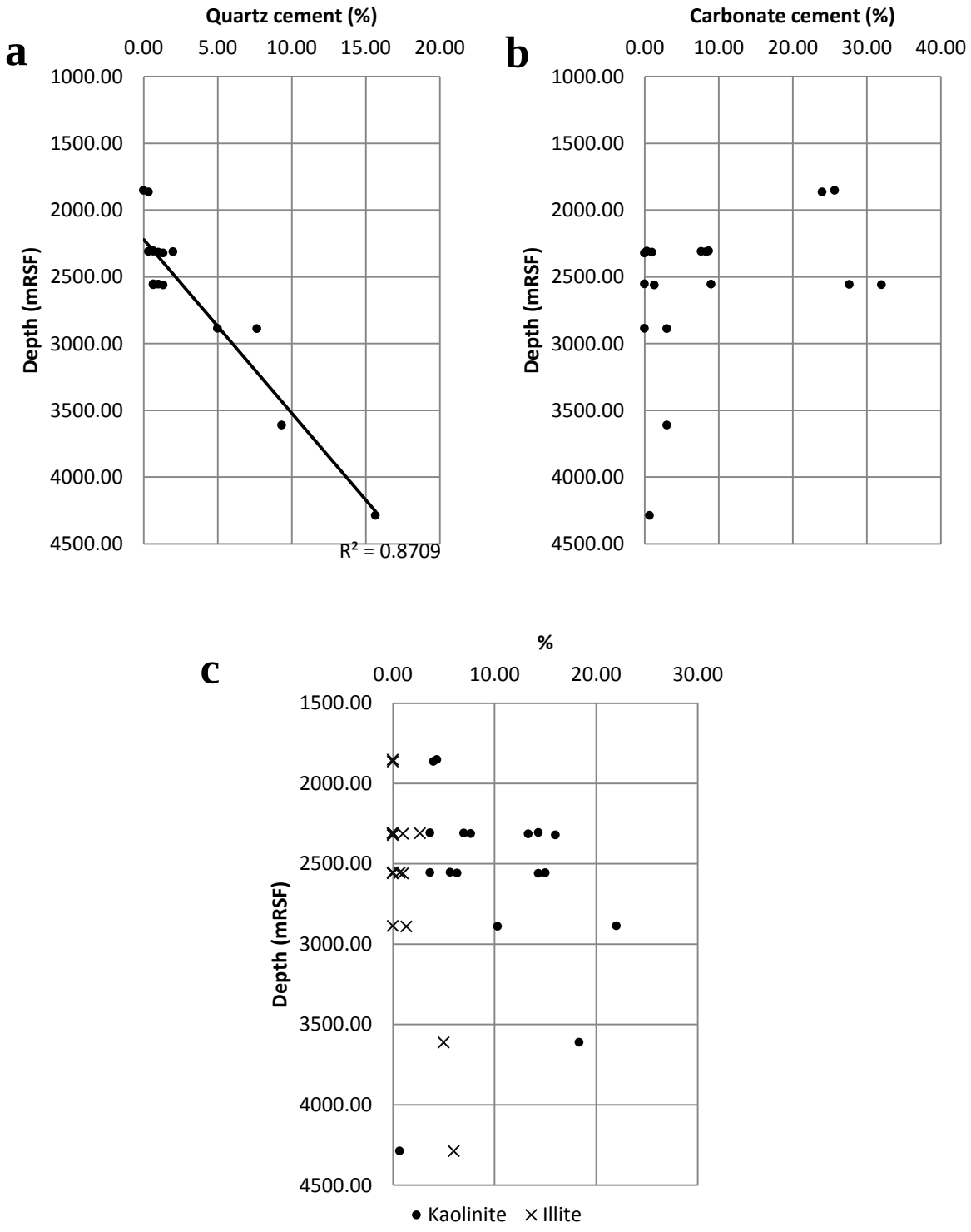

Figure 5.8: Rannoch Formation. a) Quartz cement versus depth, b) carbonate cement versus depth and c) illite and kaolinite versus depth.

5.3.1 Porosity

The porosity varies from less than 1% to 20%, with an average of 9%. The porosity is significantly lower in samples dominated by cements.

5.3.2 Intergranular volume and textural parameters

The intergranular volume (IGV) for the Rannoch Formation ranges from 18% to 44%, averaging at 31%. The average grain sizes from each sample ranges from 56 µm to 397 µm, varying from coarse silts to medium sands.

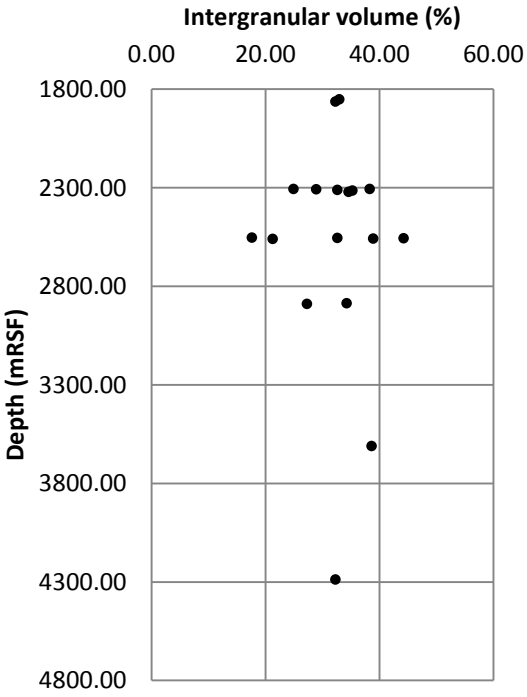

Figure 5.9: Intergranular volume versus depth in the Rannoch Formation.

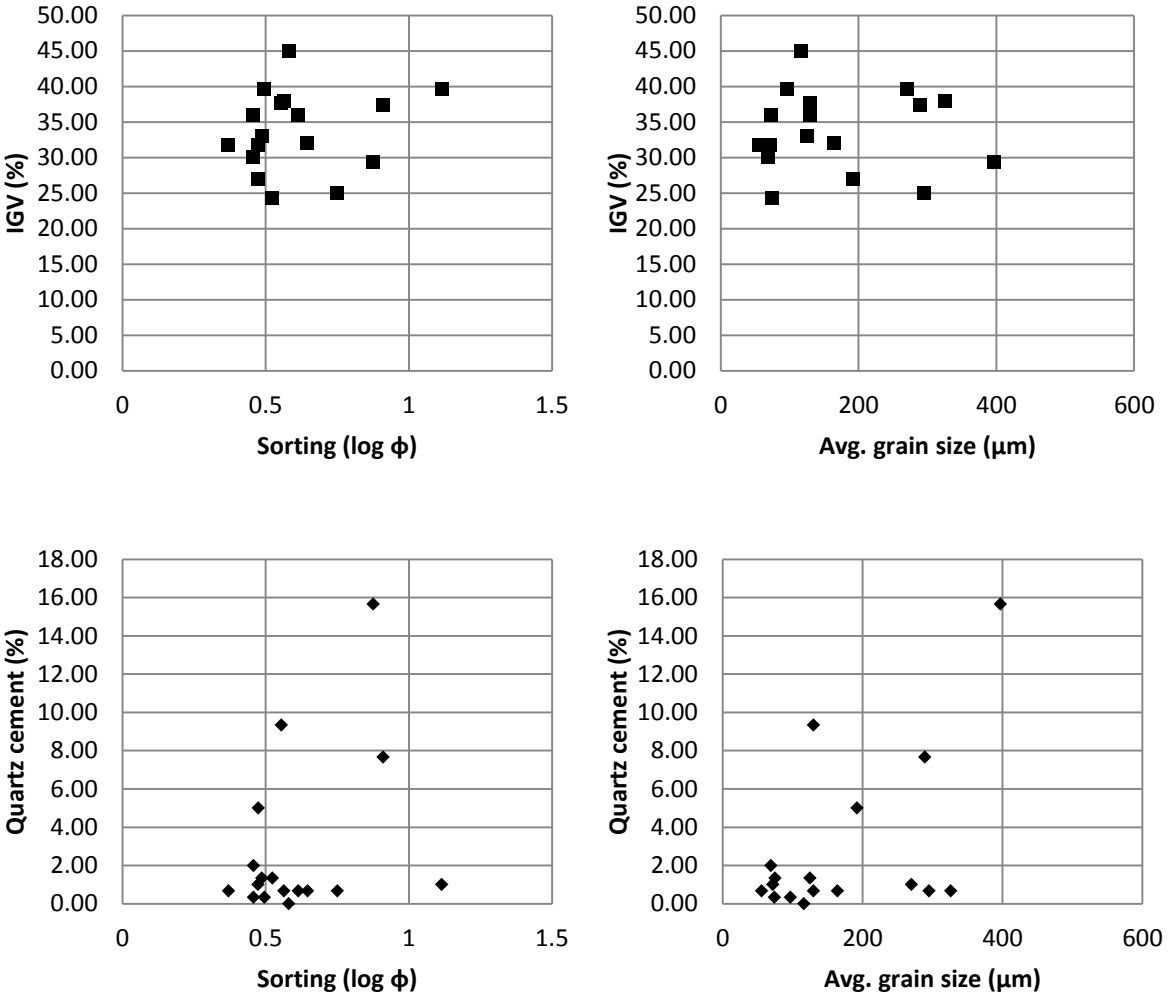

Figure 5.10: Rannoch Formation. a) IGV versus sorting, b) IGV versus average grain size, c) quartz cement versus sorting and d) quartz cement versus average grain size.

Table 5.2: The point counting results from the Rannoch Formation. All numbers are given in percentage unless specified.

Well	Depth (mRSF)	Framework				Cement					Porosity	IGV	Avg. grain size (µm)	Sorting (log φ)
		Quartz	Feldspar	Mica	Lithic fragments	Kaolinite	Illite	Chlorite	Quartz cement	Carbonate cement				
34/10-4	1852.00	53.33	11.33	1.67	0.67	4.33	0.00	0.00	0.00	25.67	3.00	33.00	116	0.58
34/10-4	1863.70	54.67	6.67	6.00	0.33	4.00	0.00	0.00	0.33	24.00	4.00	32.33	97	0.496
34/7-12	2306.00	42.00	10.33	7.33	2.00	14.33	0.00	0.00	0.67	8.67	14.67	38.33	56	0.37
34/7-12	2307.30	52.33	14.00	1.00	7.67	3.67	0.00	0.00	0.67	0.33	20.33	25.00	295	0.75
34/7-12	2309.00	44.33	15.33	11.00	0.33	7.00	2.67	0.00	0.33	7.67	11.33	29.00	74	0.457
34/7-12	2312.00	47.67	9.00	8.33	2.33	7.67	1.00	0.00	2.00	8.33	13.67	32.67	69	0.458
34/7-12	2315.15	47.00	7.67	9.33	4.33	13.33	0.00	0.00	1.00	1.00	16.33	35.33	72	0.473
34/7-12	2321.00	49.33	10.33	13.00	1.67	16.00	0.00	0.00	1.33	0.00	8.33	34.67	75	0.524
35/11-1	2553.60	70.67	10.00	1.33	0.33	5.67	0.00	0.00	0.67	0.00	11.33	17.67	326	0.564
35/11-1	2554.60	56.33	8.00	2.33	0.67	3.67	0.67	0.00	1.00	9.00	18.33	32.67	270	1.115
35/11-1	2556.60	45.33	4.67	4.33	1.33	15.00	0.00	0.00	0.67	27.67	1.00	44.33	164	0.646
35/11-1	2558.30	49.00	6.00	5.67	0.33	6.33	0.00	0.00	0.67	32.00	0.00	39.00	130	0.614
35/11-1	2560.70	65.33	1.00	8.33	4.00	14.33	1.00	0.00	1.33	1.33	3.33	21.33	125	0.487
30/3-2R	2886.50	48.00	5.67	10.67	1.33	22.00	0.00	0.00	5.00	0.00	7.33	34.33	192	0.474
30/3-2R	2889.30	60.00	7.00	2.00	3.67	10.33	1.33	0.00	7.67	3.00	5.00	27.33	289	0.91
33/6-1	3611.60	41.67	9.00	8.67	2.00	18.33	5.00	0.00	9.33	3.00	3.00	38.67	130	0.555
34/10-23	4287.65	62.67	4.33	0.00	0.67	0.67	6.00	0.00	15.67	0.67	9.33	32.33	397	0.876
Average		**52.33**	**8.25**	**5.94**	**1.98**	**9.80**	**1.04**	**0.00**	**2.84**	**8.96**	**8.84**	**31.49**	**169.24**	**0.61**

5.4 Composition and texture of the Etive Formation

Based on the point counting result in (table 5.3) the average Etive sandstone is classified as $Q_{87}F_{11}R_2$, meaning the sandstone consists of 87% quartz, 11% feldspar and 2% lithic rock fragments. Thus, the average Etive Formation sand is subarkose.

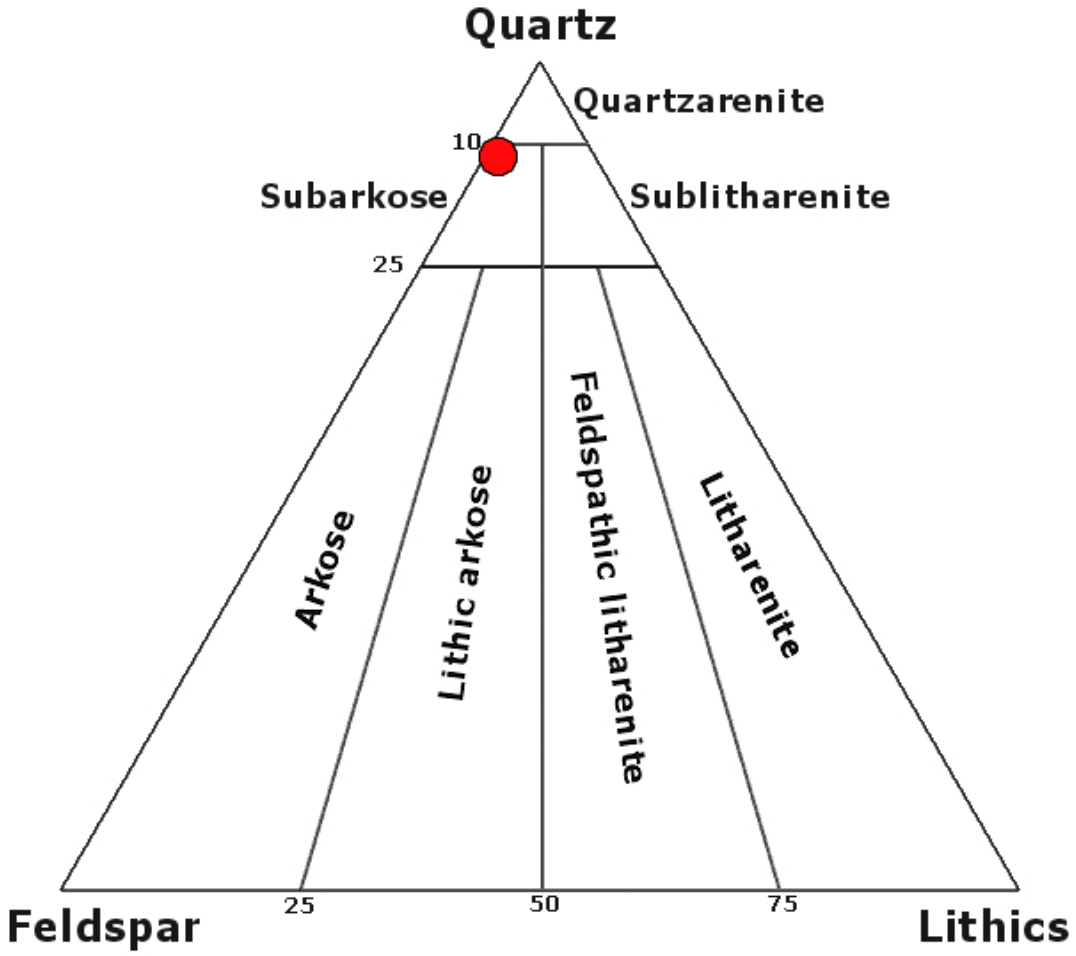

Figure 5.11: Average QFR of sandstones from the Etive Formation samples classified in Folk's classification of sandstones (Folk, 1968).

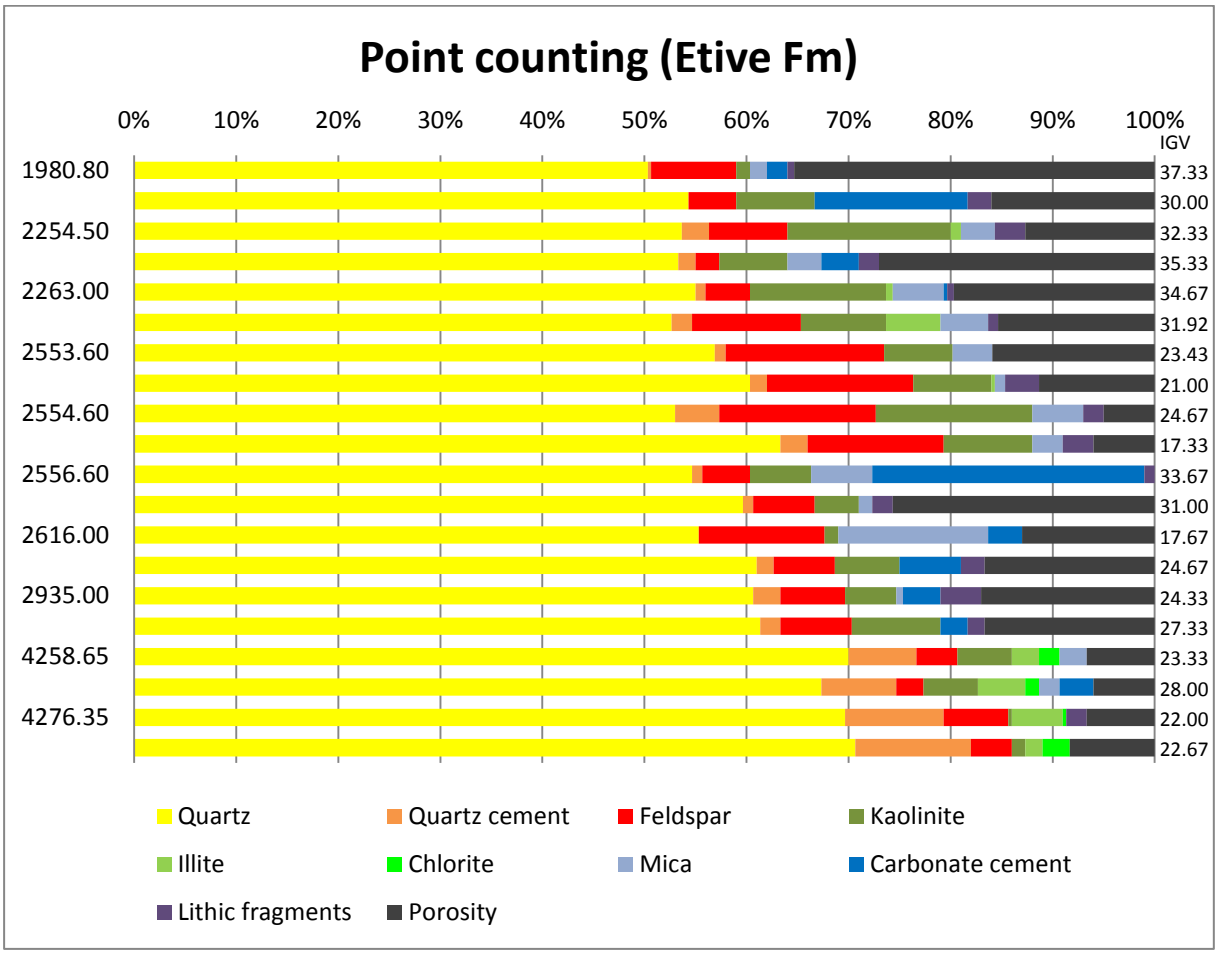

Figure 5.12: Point counting results from the Etive Formation.

5.4.1 Framework mineralogy

Quartz

Quartz grains dominate the framework with an 87% average of the framework grains and a 59% average of the total mineral composition, including the matrix. The grains are colourless and mainly angular to subangular in shape.

K-feldspar ($KAlSi_3O_8$) and albite ($NaAlSi_3O_8$)

The Etive Formation is dominated by two types of feldspar; K-feldspar and albite. Their formation and behavior has been discussed in previous chapters. The feldspar content in each of the samples ranges from 4.5% to 21.8% of the framework composition, and 2% to 15% of

the total mineral composition. The average is 7.8%. The highest amounts of feldspar are observed in samples buried 2-2.9 km.

Residual framework and detrial clays

Mica was found in 15 of 20 samples. The average mica content for the whole formation was 3%. Chlorite was only found in well 34/7-12, with an average content of 1.5%.

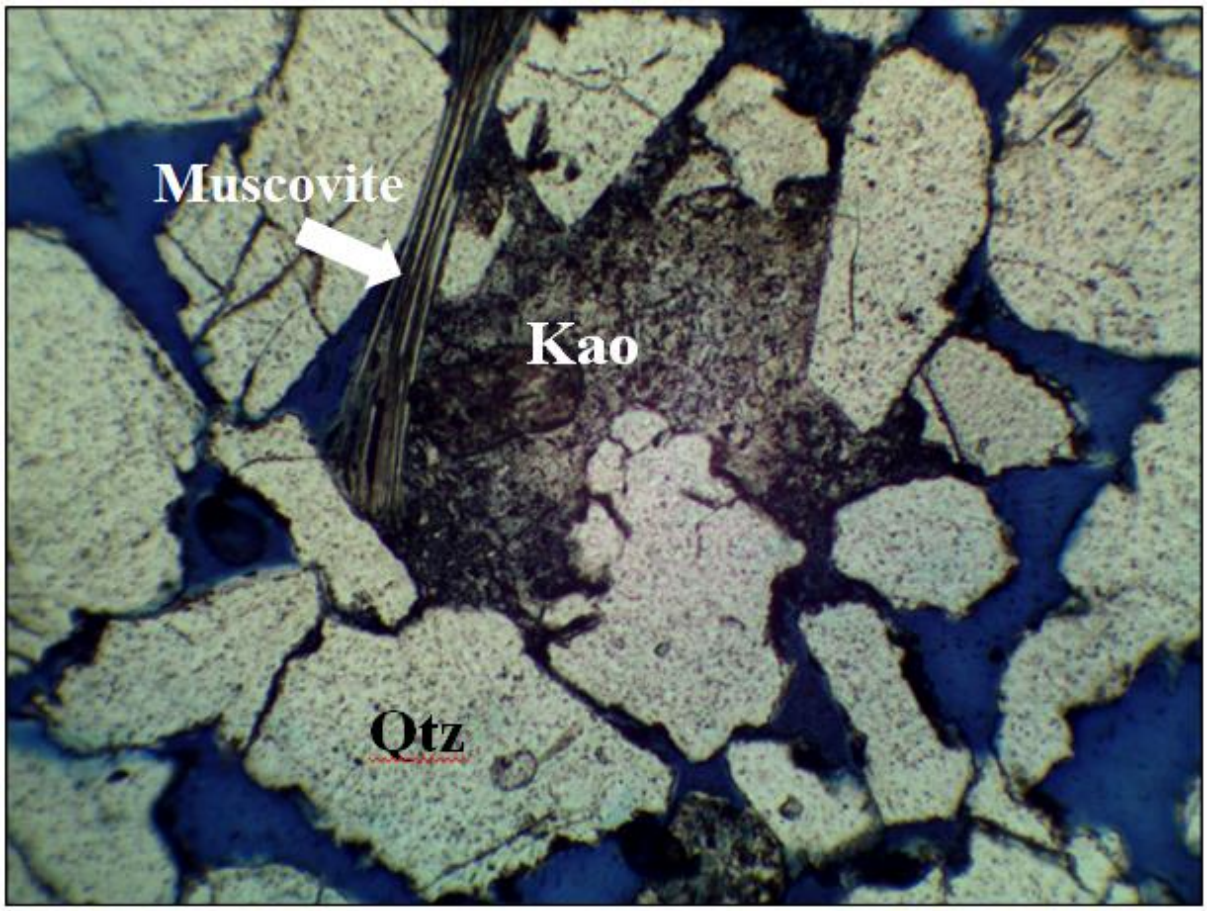

Figure 5.13: Etive Formation: kaolinite at 2934.7 m in well 34/10-17.

5.4.2 Cements

Quartz

The average quartz cement content for the whole formation is 3%. The highest amounts are found in the deepest buried samples from well 34/10-23 (4258.65 m, 4270.65 m, 4276.35 m and 4281.35 m), with an average of 9%. With no CL available, these numbers are subjects to uncertainty.

Carbonate

Carbonate cements were observed in 9/20 of the samples, with an average of 3%. The amount ranges from 0% to 27%. The degree of cementation showed no apparent correlation with depth.

Kaolinite

Kaolinite was found in all thin sections ranging from less than 1% to 16%. The average for the Etive Formation was 7%. The kaolinite amount was highest in samples buried from 2.2 km to 3 km, with an average of 8%. Well 34/7-12 had the largest kaolinite content with an average of 11%. The kaolinite was primarily pore filling, precipitated as a result of dissolved mica or K-feldspar in secondary pores.

Illite

Illite was present in 7 of 20 samples. Authigenic illite was observed in samples buried deeper than 4 km (well 34/7-12), with an average amount of 3.5%. Some of the shallower buried samples showed detrial illite grains either in or around micas.

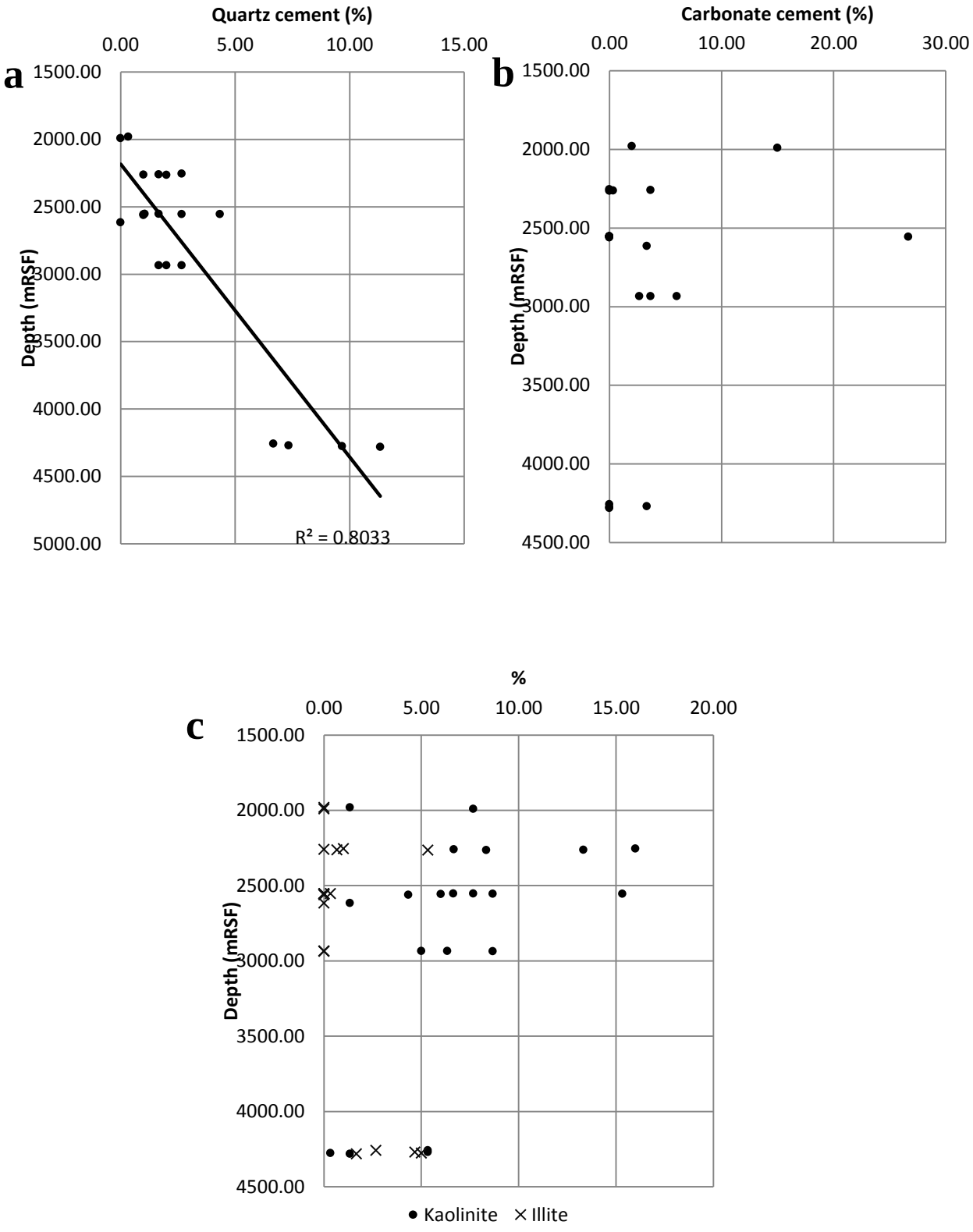

Figure 5.14: Etive Formation. a) Quartz cement versus depth, b) carbonate cement versus depth and c) illite and kaolinite versus depth.

5.4.3 Porosity

The porosity is higher in the Etive Formation when compared to Ness and Rannoch, with an average of 14%. The porosity varies from less than 1% to 35%. Note that the samples with the highest porosities may be due to poor thin section preparation.

5.4.4 Intergranular volume and textural parameters

The average IGV is 28%, varying from 17% to 39%. Two samples showed abnormally low IGV values of 17-18%.

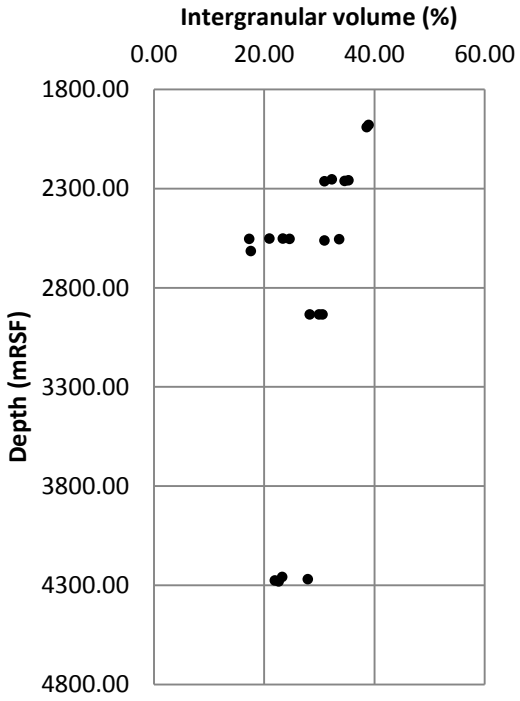

Figure 5.15: Intergranular volume versus depth in the Etive Formation

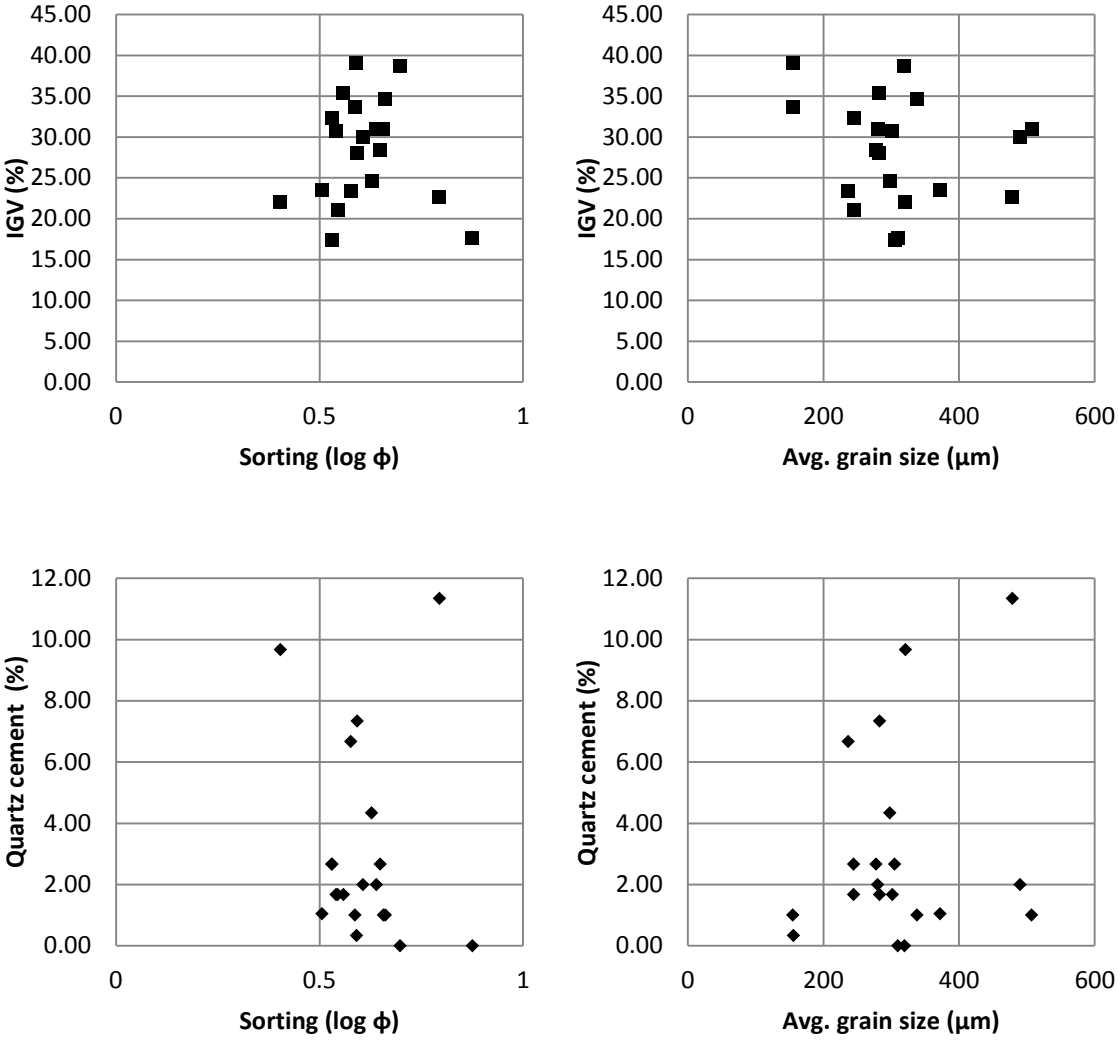

Figure 5.16: Etive Formation. a) IGV versus sorting, b) IGV versus average grain size, c) quartz cement versus sorting and d) quartz cement versus average grain size.

Table 5.3: Point counting results for the Etive Formation. The numbers are given in percentage unless specified.

		Framework				Cement								
Well	Depth	Quartz	Feldspar	Mica	Lithic fragments	Kaolinite	Illite	Chlorite	Quartz cement	Carbonate cement	Porosity	IGV	Avg. grain size (μm)	Sorting (log φ)
34/10-3	1980.80	50.33	8.33	1.67	0.67	1.33	0.00	0.00	0.33	2.00	35.33	39.00	156	0.591
34/10-3	1991.48	54.33	4.67	0.00	2.33	7.67	0.00	0.00	0.00	15.00	16.00	38.67	320	0.698
34/7-12	2254.50	53.67	7.67	3.33	3.00	16.00	1.00	0.00	2.67	0.00	12.67	32.33	245	0.531
34/7-12	2260.00	53.33	2.33	3.33	2.00	6.67	0.00	0.00	1.67	3.67	27.00	35.33	283	0.559
34/7-12	2263.00	55.00	4.33	5.00	0.67	13.33	0.67	0.00	1.00	0.33	19.67	34.67	338	0.662
34/7-12	2264.00	52.67	10.67	4.67	1.00	8.33	5.33	0.00	2.00	0.00	15.33	31.00	280	0.64
35/11-1	2553.60	56.29	15.38	3.85	0.00	6.64	0.00	0.00	1.05	0.00	15.73	23.43	372	0.506
35/11-1	2553.60	60.33	14.33	1.00	3.33	7.67	0.33	0.00	1.67	0.00	11.33	21.00	245	0.545
35/11-1	2554.60	53.00	15.33	5.00	2.00	15.33	0.00	0.00	4.33	0.00	5.00	24.67	298	0.628
35/11-1	2554.60	63.33	13.33	3.00	3.00	8.67	0.00	0.00	2.67	0.00	6.00	17.33	305	0.531
35/11-1	2556.60	54.67	4.67	6.00	1.00	6.00	0.00	0.00	1.00	26.67	0.00	33.67	155	0.587
30\6-10	2561.87	59.67	6.00	1.33	2.00	4.33	0.00	0.00	1.00	0.00	25.67	31.00	507	0.657
33/9-3	2616.00	55.33	12.33	14.67	0.00	1.33	0.00	0.00	0.00	3.33	13.00	17.67	310	0.876
34/10-17	2934.70	61.00	6.00	0.00	2.33	6.33	0.00	0.00	1.67	6.00	16.67	30.67	302	0.541
34/10-17	2935.00	60.67	6.33	0.67	4.00	5.00	0.00	0.00	2.67	3.67	17.00	28.33	278	0.649
34/10-17	2935.60	61.33	7.00	0.00	1.67	8.67	0.00	0.00	2.00	2.67	16.67	30.00	490	0.607
34/10-23	4258.65	70.00	4.00	2.67	0.00	5.33	2.67	2.00	6.67	0.00	6.67	23.33	237	0.577
34/10-23	4270.65	67.33	2.67	2.00	0.00	5.33	4.67	1.33	7.33	3.33	6.00	28.00	283	0.593
34/10-23	4276.35	69.67	6.33	0.00	2.00	0.33	5.00	0.33	9.67	0.00	6.67	22.00	321	0.404
34/10-23	4281.35	70.67	4.00	0.00	0.00	1.33	1.67	2.67	11.33	0.00	8.33	22.67	479	0.795
Average		**59.13**	**7.79**	**2.91**	**1.55**	**6.78**	**1.07**	**0.32**	**3.04**	**3.33**	**14.04**	**28.24**	**310.20**	**0.61**

5.5 SEM analysis of the Ness Formation

5.5.1 Porosity

In the majority of the studied samples, K-feldspar was either present or dissolved and replaced by either kaolinite or illitized kaolinite (fig 5.17 & 5.18). Albite was also observed to have replaced K-feldspar in many of the samples (fig 5.17). In the shallower buried samples, much of the initial porosity was replete with carbonate cement. Area measurements show that the porosity can be as high as 21% in the deepest buried samples (measured on a 4 mm^2 surface at 4241.6 m in well 34/10-23).

5.5.2 Clays

Kaolinite is often observed in areas with secondary porosity. Kaolinite formed by muscovite-transformation is also common throughout the formation. Illite or partly illitized kaolinite is more frequent with depth (fig 5.14). The illite resembles kaolinite morphologically in some areas, but is easily recognized in areas where it has formed into its characteristic fibrous morphology. Quartz cement is often found to grow around the illite in areas where the illite is formed near a quartz surface.

Chlorite grains are often observed in a state where its sheets are separated or partly separated.

5.5.3 Other cements

Quartz

With no CL to distinguish quartz from quartz cement there is no convenient way to use the SEM to acquire an approximate volume of quartz cement. Quartz overgrowth is therefore only observed by studying the morphology of the grain surfaces. This is again done solely by studying thin sections, as no core sands were available. This excludes the possibility of observing microquartz on the grain surfaces. Samples buried deeper than 4 km were used to study quartz cementation. The quartz grains with surrounding cement are often straight lined. The cement may grow evenly across the surface, or in some areas grow outwards as small peninsulas. Illite is often found along the edges, or even within the growth direction of the cement (see fig 5.19). No other coatings were observed in the thin sections.

Carbonate

Authigenic carbonate crystals are observed in the form of Mg-rich siderite. Many samples contain calcite in the form of cement. No ankerite was observed in the studied samples of the Ness Formation. Calcite cement is found between grain surfaces, but is not seen in areas of precipitated kaolinite. This indicates that the process of calcite cementation postdates formation of authigenic clays.

Pyrite

The Ness Formation distinguishes itself in the fact that there is a lot more pyrite cement present here, than in both the Etive and the Rannoch formations. The pyrite is observed within mica grains, among kaolinite and illite, as well as in bigger clusters (fig 5.19).

5.5.4 Other

Titanium oxides (rutile and anatas) and zircon were observed in small quantities. No coatings were observed.

Text to figure 5.17-5.19

5.17: Pore-filling kaolinite at 2850.5 m in well 30/3-3 in the Etive Formation. The denser grains (white) mainly grains of pyrite, found in between crystals of kaolinite and in muscovite, and titanium oxides. Chlorite is observed in many samples, contrary to the point counting (see b). Albite is also present, though hard to separate from quartz due to similar density and morphology (see c).

5.18: (4241.65 m). a) Illitized kaolinite formed by muscovite-transformation. Smaller grains of siderite are also present. b) Illite formed by mica and kaolinite, and rutile.

5.19: a) and b) Illite limiting the growth of quartz cement (4241.65 m). c) Calcite cement at 2850.4 m. d) Pyrite cement at 2885.0 m.

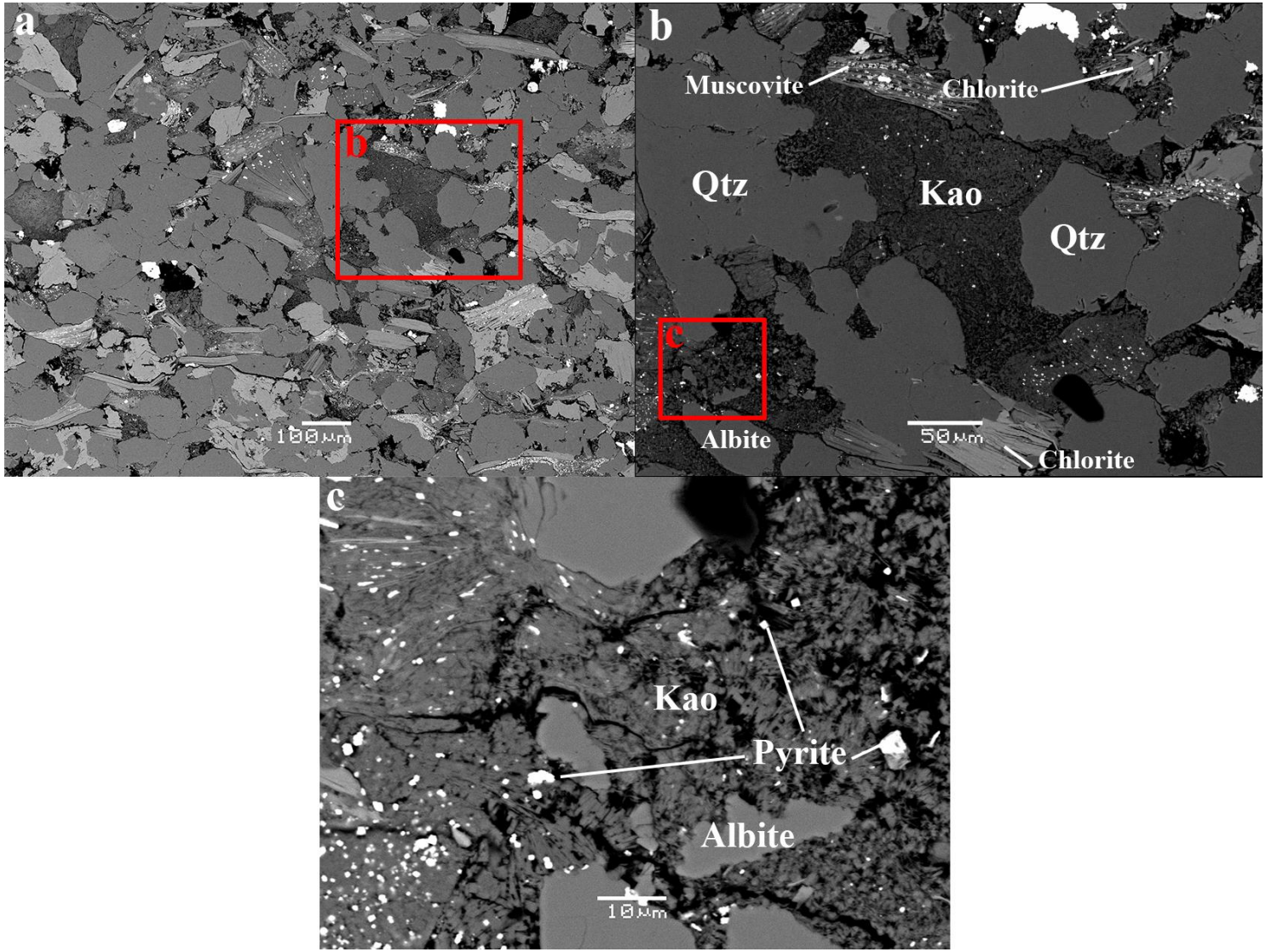

Figure 5.17: See text on page 64.

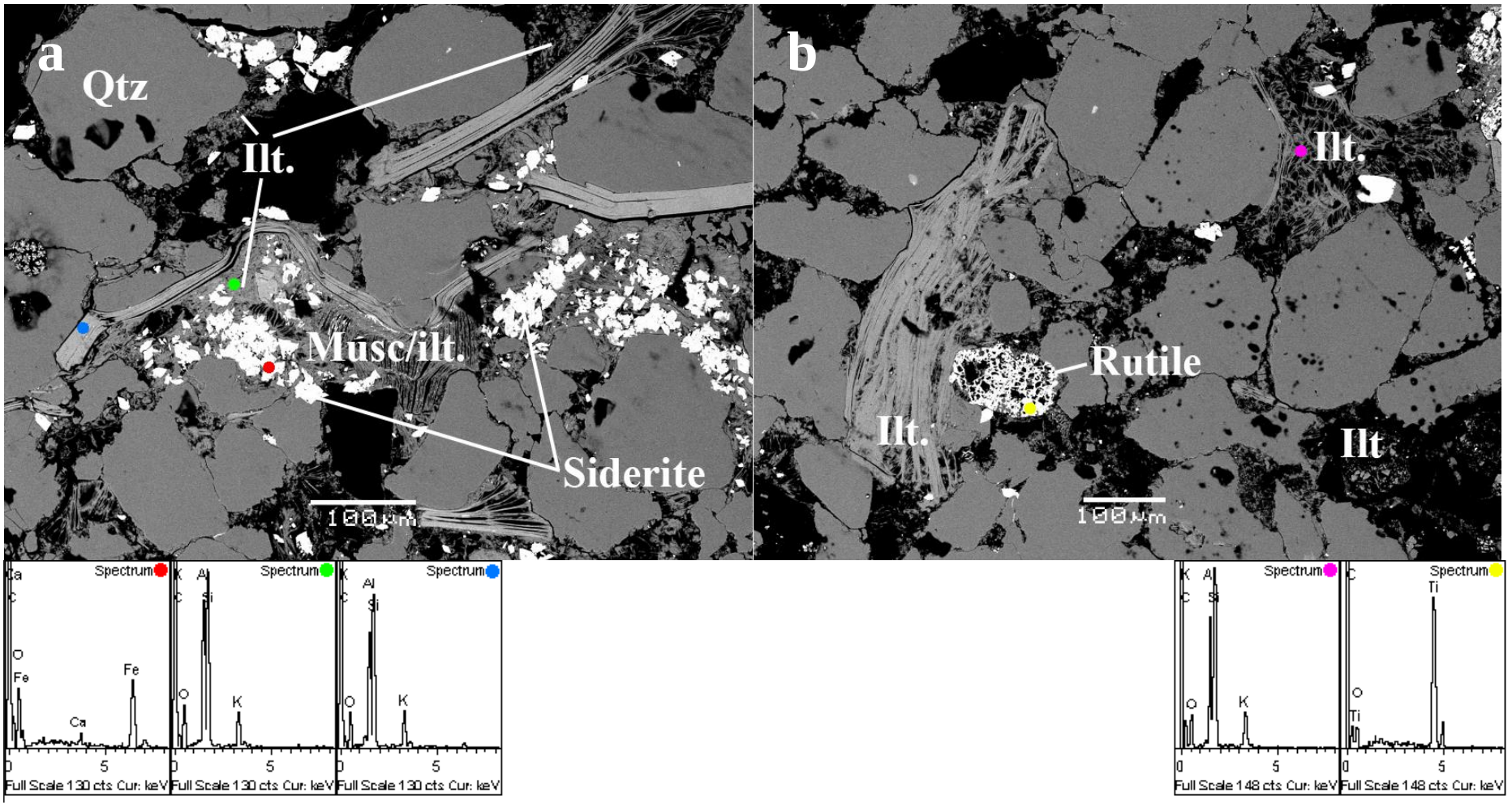

Figure 5.18: See text on page 64.

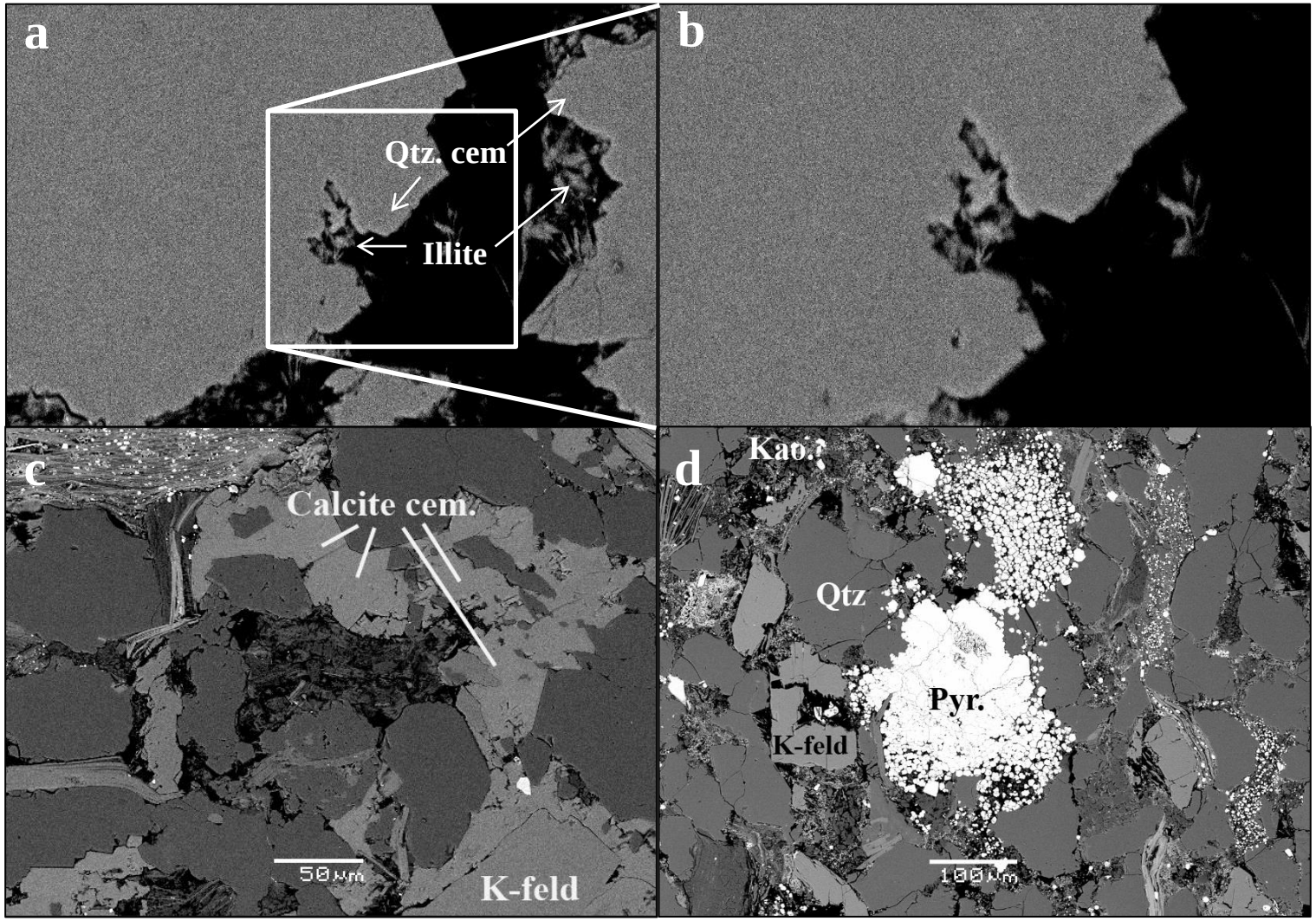

Figure 5.19: See text on page 64.

5.6 SEM analysis of the Rannoch Formation

5.6.1 Porosity

The porosity in the Rannoch Formation varies greatly. The samples with low porosity generally have a higher content of cements, especially carbonate. Area measurements of sample 1863.7 m in well 34/10-4, show a local (2.4 mm^2) porosity up to 9.8%. Another area measurement of sample 3611.6 m well 33/6-1, show a porosity level of 10%.

5.6.2 Clays

Kaolinite was observed in all of the studied samples. The amount of kaolinite varied significantly between and within each well. Variations in kaolinite content up to 400% were observed in well 34/7-12. Illite was predominantly observed in the one sample below 4 km (at 4287.65 m).

Chlorite was mainly observed as randomly dispersed grains. In some samples, there was evidence of sorting with respect to density, where heavy minerals were sorted in rows between the lighter minerals (fig 5.21).

5.6.3 Other cements

Quartz

As no CL was available, the volume of quartz cement is uncertain. Other than the morphology of quartz cemented grains, and to some degree the ratio between quartz volume and porosity, it is difficult to establish the level of quartz cementation. The samples from 3611.6 m and 4287.65 m both showed classical signs of cementation (i.e. straight edges, small outgrows), 4287.65 m more so than 3611.65 m (fig 5.20).

Carbonate

Crystals of authigenic Mg-rich siderite were observed in clusters in samples buried deeper than 3 km. Pore-filling calcite cement was observed in 2 of the 4 SEM analyzed samples, at 1863.7 m and 3611.6 m (fig 5.20).

5.6.4 Other

The mica content, as mentioned in the optical microscopy section, was high in some samples. In the sample from 2321.0 m, one could clearly see that the mica and chlorite grains were sorted together in in rows (5.21).

No coatings were observed.

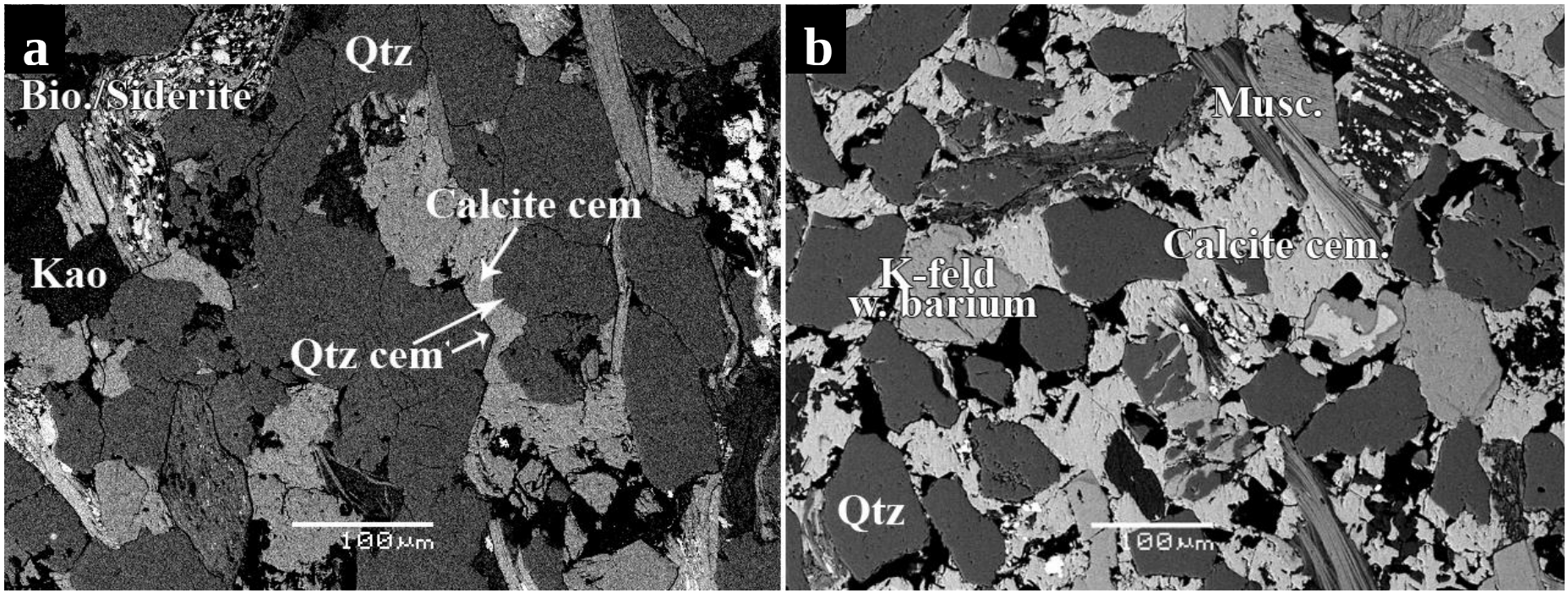

Figure 5.20: a) 3611.6 m: quartz and calcite cemented sandstone. Heavy altered biotite with siderite, b) 1863.7 m: heavily calcite cemented sandstone. K-feldspars from this sample often contained barium in its core

.

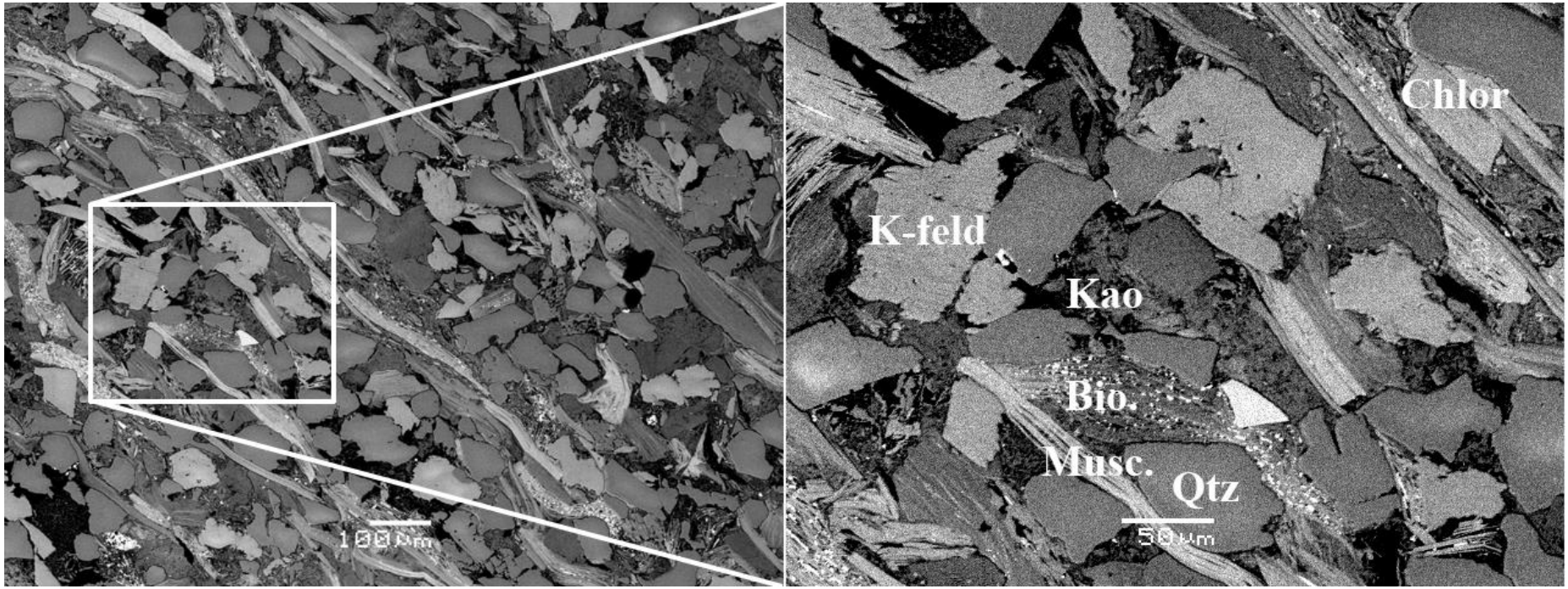

Figure 5.21: 2321.0 m: a) Sandstone with high content of sorted mica and chlorite, b) K-feldspar, biotite, muscovite, chlorite, quartz and kaolinite.

5.7 SEM analysis of the Etive Formation

5.7.1 Porosity

Area measurements show that the porosity can be as high as 31% in some of the shallower buried samples (measured at 2260.0 m in well 34/7-12). Such high porosity sands are exclusively observed in samples containing low amounts of cement. The samples from the Etive Formation have lower average carbonate cement content than both Ness and Rannoch. Secondary porosity is, similarly to the Ness Formation, seen in areas of dissolved K-feldspar.

5.7.2 Clays

Kaolinite is the dominant clay in samples buried < 4 km. Kaolinite was, however, found in samples > 4 km, but in substantially less amounts. The sheer amount of kaolinite is shown to vary greatly, even within the same well. Kaolinite formed by muscovite-transformation can be seen in figure 5.22b. Kaolinite formed with K-feldspar as a reactant can be seen in figure 5.22a.

Illite or illitized kaolinite was predominantly found below 4 km. In one sample at 4270.65 m, illite was observed to co-exist side by side with kaolinite. In these areas, there were no reactants such as muscovite or K-feldspar present (fig. 5.22c & d). How much pore space the illite occupies is varying from less than 10% to almost 100%.

Compared to the Ness Formation, there were considerably less illite present in the deeply buried samples (> 4 km).

5.7.3 Other cements

Quartz

Samples buried deeper than 4 km appear heavily quartz cemented, maybe even more so than stated in the point counting. The sheer volume was, however, not measured due to the fact that the CL was out of order.

Carbonate

Both crystals of authigenic Mg-rich siderite and more Fe-rich ankerite are observed in samples buried deeper than 4 km. The siderite is often observed in clusters, as authigenic rhombs within a limited area or as cement (fig, 5.23a). Rhombs of siderite were also observed in micas (fig. 5.22b). Ankerite is mainly observed as pore-filling cement in samples < 4 km. The authigenic crystals found >4 km has a higher density than the cements.

Compared to both the Ness and the Rannoch formations, there are less carbonate cement observed in the Etive Formation.

5.7.4 Other

Iron oxide, anatas and zircon were observed in small quantas. No coatings were observed.

5.7.5 Text to figure 5.22

5.22: a) 2260.0 m: Formation of kaolinite from dissolved K-feldspar. Note that there are still small grains of K-feldspar present. **b)** 2556.6 m: Kaolinite formation by muscovite-transformation (top). The denser (brighter) phyllosilicate is chlorite. Rhombs of Mg-rich siderite is observed within both muscovite and chlorite grains. **c)** and **d)** 4270.65 m: Most of the kaolinite has been illitized. Note that in c) there are both kaolinite and pore-filling illite present in close proximity.

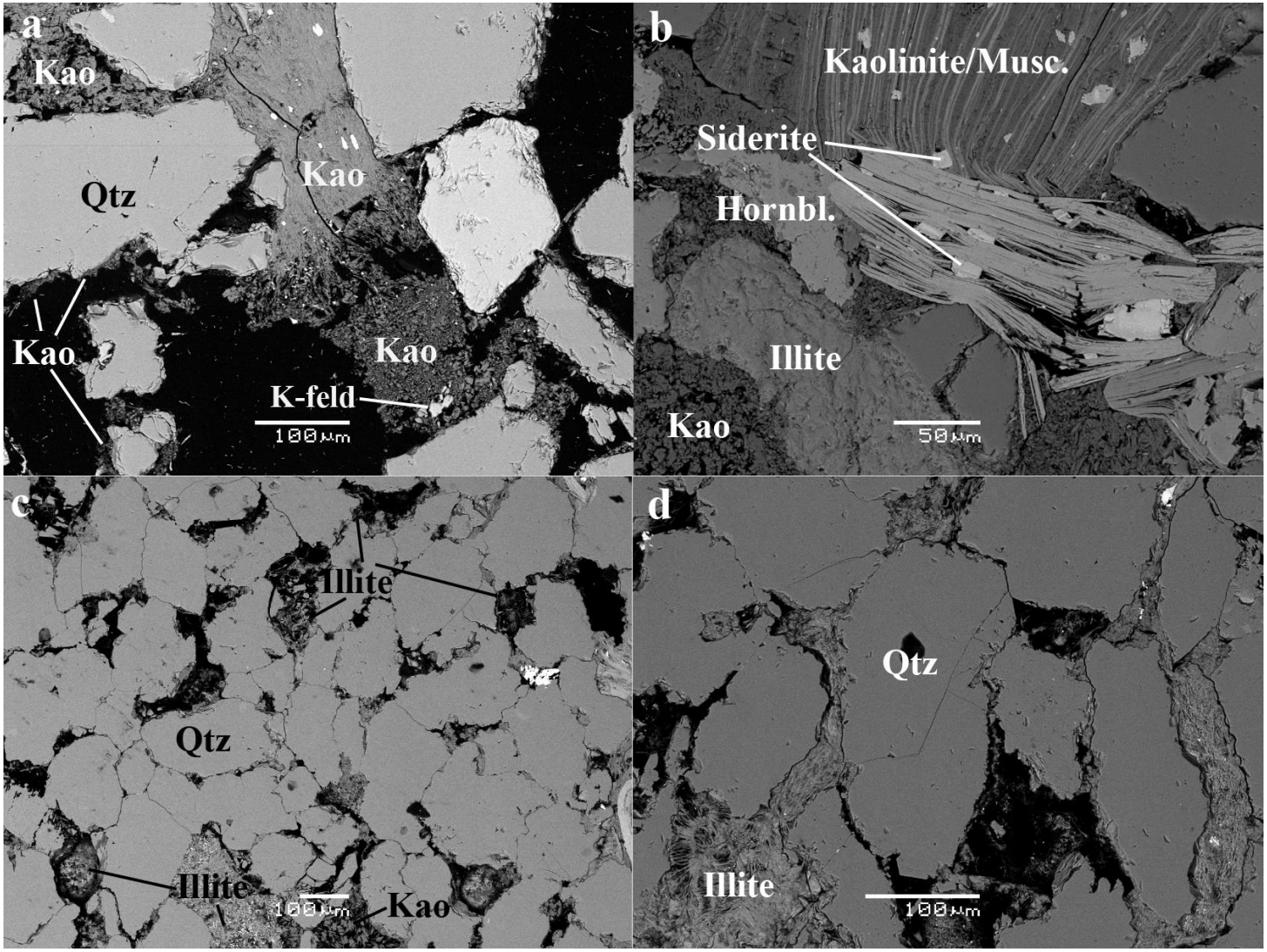

Figure 5.22: see text to figure on page 73.

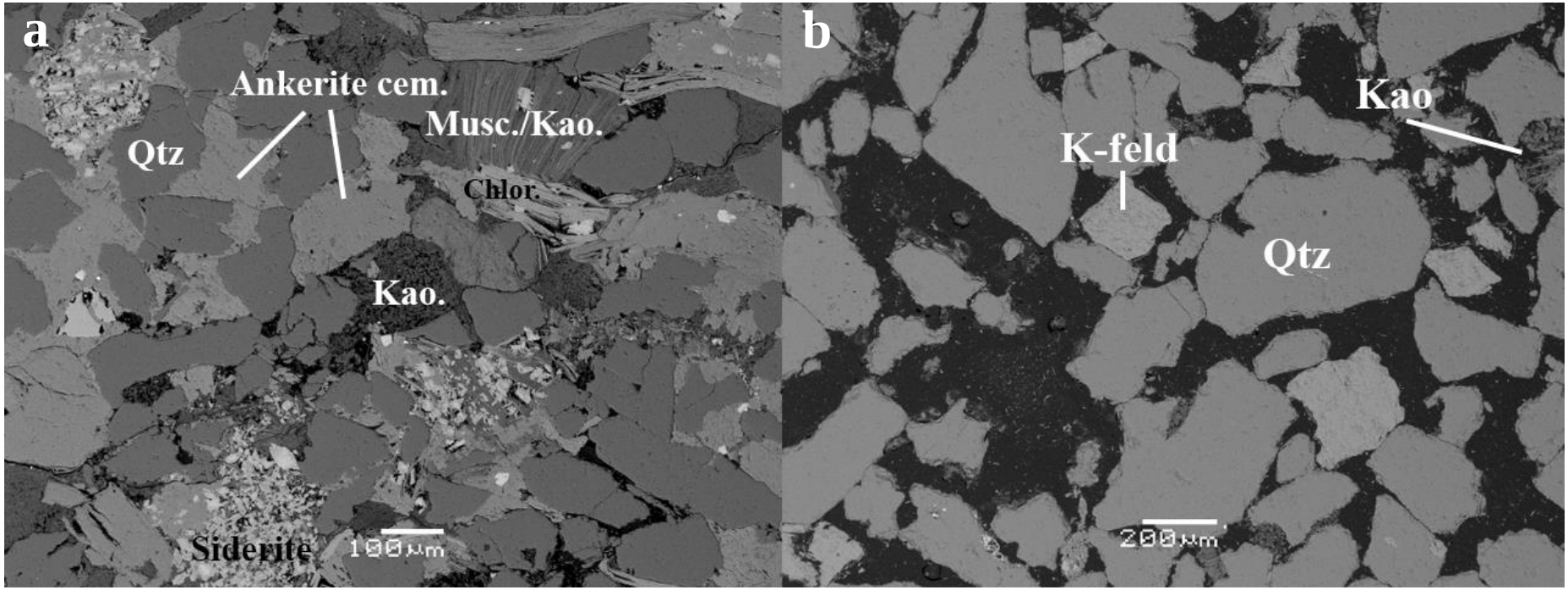

Figure 5.23: Difference in porosity between a carbonate cemented sandstone (a) and a sandstone with low content of carbonate cement (b). Sample; a) well 35/11-1 2556.6 m; b) well 34/7-12 2260.0 m.

6 Discussion

6.1 Mineral assemblage and early diagenesis

6.1.1 Framework minerals and deposition

The sandstones of the Etive, Ness and Rannoch formations are rather similar in terms of framework minerals. Of the studied samples, the main difference is found in the ratio of quartz to feldspar (Q/F). The variation in lithic rock content among the three is negligible, separated by only 1%. None of the formations contain more than 3% lithic rock fragments. The Ness sandstone has the least amount of feldspar. With a quartz content of over 90%, it is classified as a quartzarenite. Samples from the Rannoch and Etive formations contain less quartz and more feldspar, and therefore classifies as subarkoses.

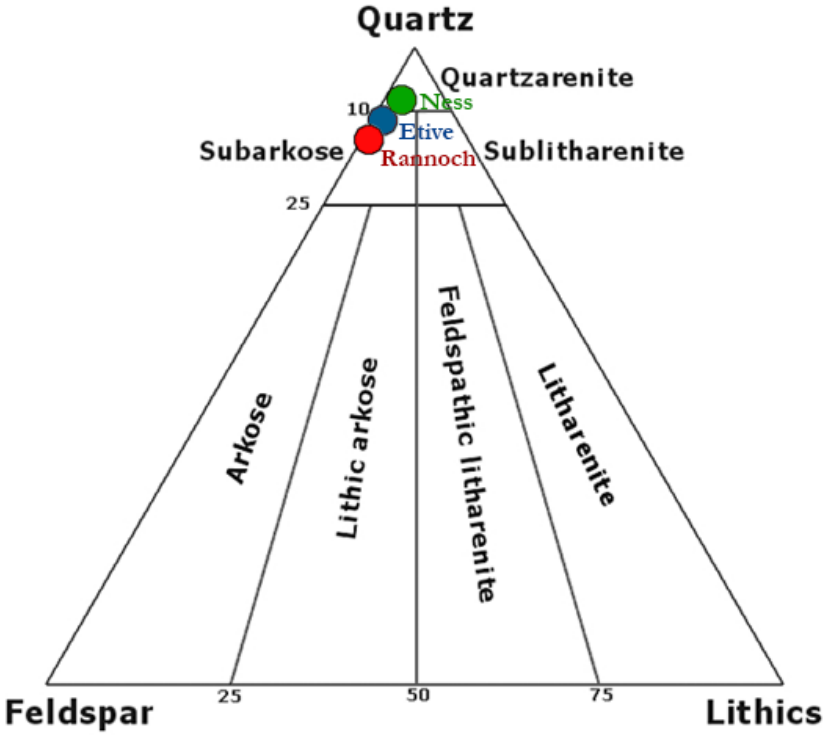

Figure 6.1: Classification of the Etive, Ness and Rannoch sandstones in a QFR diagram.

The different Q/F ratios may be a result of several factors. Feldspars must be deposited rapidly in order to avoid significant chemical weathering. Rework, leaching, sedimentation rate and climate may all influence weathering of feldspars.

In sandstones, leaching of K-feldspars by meteoric water may lead to a net increase of porosity (secondary porosity). The potential of leaching by meteoric water as a means of increasing net porosity of shallowly buried sandstones is of relevance for hydrocarbon

production, as a way of increasing permeability and porosity in sandstone reservoirs (Ehrenberg, 1991b, Emery et al., 1990). The secondary porosity is subject to kaolinization. This process happens during early diagenesis, in areas affected by K-feldspar dissolution, at temperatures commonly around 25°C. It is possible that part of the kaolinite described in this study is dickite. Dickite shares the same composition as kaolinite, but is in literature described as thicker and blockier. These are hard to distinguish in thin sections, so kaolinite and dickite will both be described as kaolinite in this study.

Table 6.1: Depositional environments of the Ness, Etive and Rannoch formations, sorted by proximity.
* The Rannoch Formation is interpreted differently in literature. Some interpret it as a more distal, middle/lower shoreface environment.

Proximity ↑

Formation	Depositional env.
Ness	Lower delta plain
Rannoch*	Delta front/prograding shoreface
Etive	Upper shoreface

Ness Formation

The Ness Formation is the most proximal formation, interpreted as a lower delta plain (Richards, 1992). The low feldspar content suggests that the sediments have been subject to leaching by meteoric water shortly after deposition. Heavy leaching allows more kaolinization of K-feldspars, which should normally be reflected by a higher content of kaolinite relative to feldspar in the sandstones. However, precipitation of kaolinite is also dependent on other factors. Silica released from the feldspar dissolution must also be flushed away in order for kaolinite to form. If the pore-water becomes supersaturated with silica, kaolinite will become unstable and smectice will precipitate instead. This is, however, not associated with well meteorically flushed depositions.

The point counting shows the ratio of deposited feldspar to precipitated kaolinite in the Ness Formation (F/K) to be 1:1.5. The lower amount of feldspar and the low F/K ratio suggest that the sediments from the Ness Formation have been well flushed. Kaolinite is a very resistant mineral usually formed under temperate/tropical and humid conditions. The warm and moist climate during the Middle Jurassic was therefore suitable for the precipitation of kaolinite in

relatively high amounts. Its stability and resistance means that kaolinite may be eroded from older strata and reworked into younger sediments.

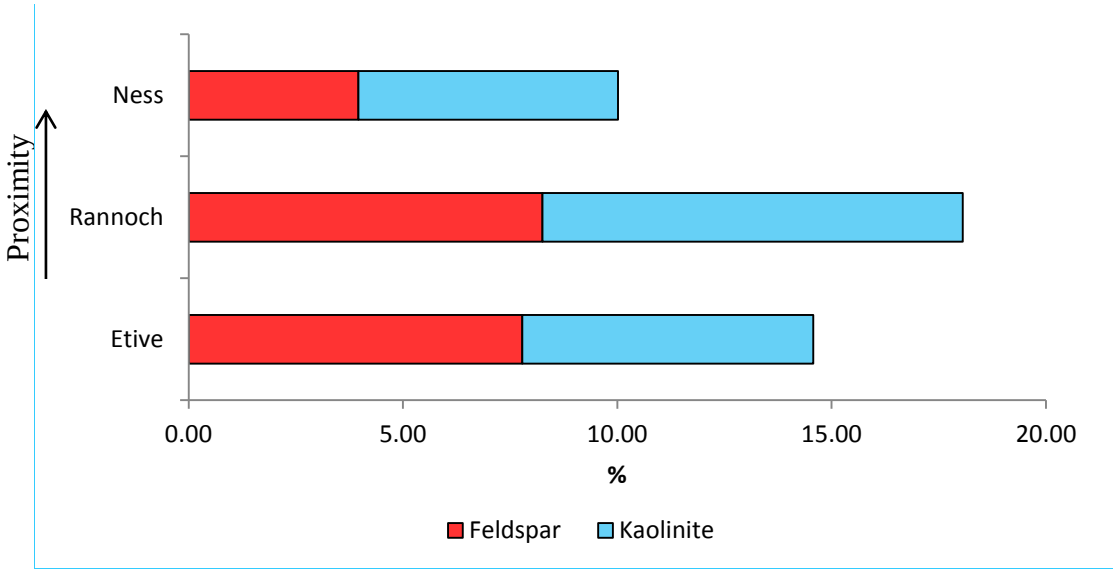

Figure 6.2: Amount and relationship between feldspar and kaolinite in all three formations.

Rannoch Formation

With a QFR ratio of 8% feldspar, the Rannoch Formation has the highest amount of feldspar as well as kaolinite. The higher F/K-ratio (fig. 6.2) and lesser proximity to the sediment source suggest that the potential for leaching is less than in the Ness Formation. The higher feldspar and mica content, and the fact that the mica in individual samples shows evidence of tidal/wave sorting (fig 5.22) suggest that the Rannoch Formation sediments were dumped in a wave energy environment and deposited rapidly. Surlyk (1991) show fluctuating sea levels on the coast of Greenland during Late Toarcian to Bajocian (fig. 3.3), with a suggested major sea level fall during Aalenian. The sea level drop is also recognized in Argentina and Tibet (Hallam, 1988, Xiaochi and Grant-Mackie, 1993). During lowstands, when the slope of the ground water table is high, the deposits may be subject to heavier leaching than normal. A reworking of these sediments could release kaolinite, and contribute this kaolinite to adjacent clay. This could explain the high amounts of kaolinite in the Rannoch Formation.

Etive Formation

The F/K ratio is highest in the Etive Formation, which is also interpreted to be the most distal of the three formations. It is the only formation where the feldspar content exceeds the precipitated kaolinite. The high F/K ratio indicates less leaching than in the Ness and Rannoch Formations. The high energy environment of the upper shoreface exposes the sediments to erosion. It is therefore likely that the sediments have been reworked with respect to kaolinite.

Figure 6.2 shows a good correlation between F/K-ratio and proximity. The rising F/K ratio with distance from the sediment source, confirms that the potential for leaching declines distally. This is also evidence that kaolinite is formed early during diagenesis.

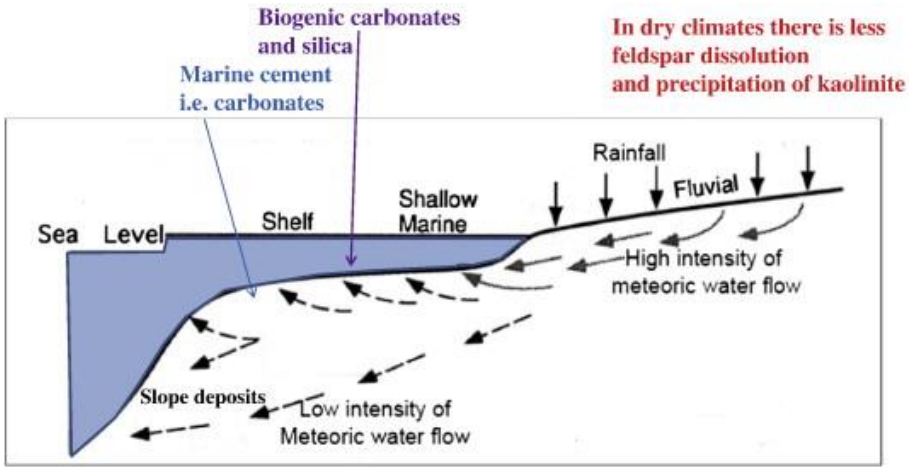

Figure 6.3: Illustration of meteoric water flow in different depositional environments. After Bjørlykke (2013).

6.1.2 Residual Framework

Previous works show that mica is a characteristic and important component in the Brent Group, especially in the Rannoch and Ness formations (Bjørlykke and Brendsdal, 1986). In this study, the Rannoch Formation contains on average twice the amount of mica compared to the Etive and Ness formations. Pore-filling kaolinite is known to occur as a result of alteration of mica and feldspar. Mica content may therefore have a significant impact on reservoir quality. Kaolinite formed as a result of mica replacement is seen in all three formations (i.e. fig. 5.23b), but to a lesser degree in the Etive and Ness formations. Mica may be a good precursor for kaolinite content, as the point counting implies a higher content of kaolinite in the Rannoch Formation than in the other two formations (see table 5.1, 5.2 & 5.3). SEM analyses show that mica buried deeper than 3.5 km is also associated with illite (fig. 5.18b). Mica will replace some of its potassium (K^+) and replace it with water. This leads to formation of some illite from mica in deeply buried sandstones (Bjørlykke and Brendsdal, 1986). Mica has in several samples shown to dissolve quartz along grain contacts, releasing silica. This process is noticeable in the deeply buried sandstones of the three formations, and is likely a source of silica for quartz cementation.

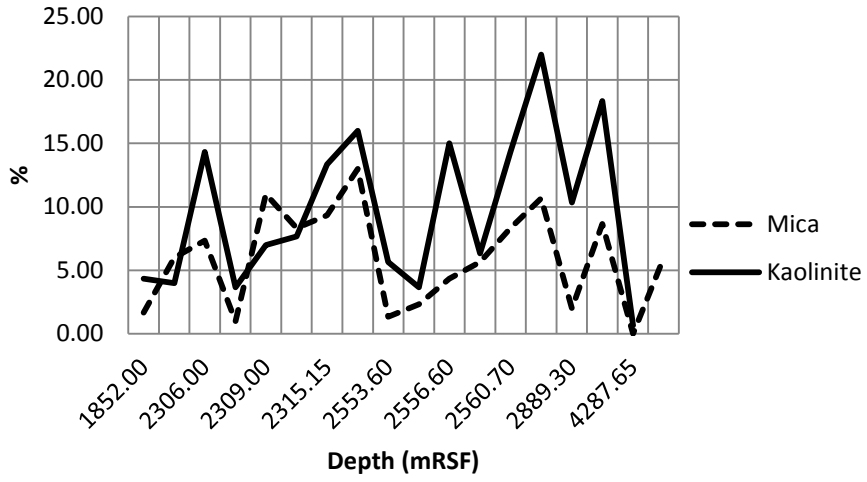

Figure 6.4: Mica and kaolinite content versus depth in the Rannoch Formation. Note the correlation between the mica and kaolinite content in some of the samples.

6.2 Major diagenetic controls

6.2.1 Quartz cementation

Quartz cement is responsible for most of the porosity loss at deeper burial (3.5 – 4.5 km). In the Etive Formation the percentage of quartz cement increases from 1 - 2% at 2.5 km to more than 11% in one sample at 4.3 km. In the Rannoch and Ness formations, the leap is even bigger, increasing from 1% at 2.5 km to more than 15% in individual samples at 4.2 - 4.3 km.

When comparing the amount of quartz cement to the level of sorting, the quartz cement in the Ness Formation shows a slight tendency to increase with well sorted sediments. In the Etive and Rannoch formation, the amount of quartz cement shows little correlation with sorting. A greater number of quartz cemented thin sections are required to conclude any assumptions.

When comparing the level of quartz cement to grain size, the data is also inconclusive. Samples from the Ness Formation show a clear trend of increasing quartz cementation with finer grain sizes. Samples from the Etive Formation show no clear trend, while samples from the Rannoch Formation shows slightly increased quartz cementation with coarser grain size. Studies show that intervals of finer grain sizes tend to be more heavily quartz cemented, because of the increased surface area per volume of quartz (Bjørlykke and Brendsdal, 1986, Bjørlykke et al., 1992, Walderhaug, 1996, Walderhaug and Bjorkum, 2003). However, as discussed by McBride (1989), some researchers have reported opposite findings, indicating that the amount of surface area may also depend on other factors than grain size.

It is unlikely that the water flow 3-5 km beneath the seafloor is significant enough to transport adequate silica to be responsible for the heavily cemented, deeply buried sediments (Bjørlykke et al., 1992). Although no stylolites were observed in the few studied samples buried deeper than 3 km, the source of silica for the quartz cement in all formations may be explained by pressure solution from both grain contacts and stylolites. The high intergranular volume coupled with the high amount of quartz cement found in all formations is an indicator of stylolites. Some silica is also released during leaching of mica and feldspar, and during kaolinization of illite (Bjørlykke and Aagaard, 1992). An abundance of mica, such as observed in the Rannoch Formation, may increase cementation in sediments buried <3 km, due to quartz being dissolved at mica-quartz grain contacts. In the Rannoch Formation, volumes of quartz cement up to 7.5% were observed in individual samples buried shallower

than 3 km. Some of the samples from the Rannoch Formation show evidence of wave sorting (fig. 5.22). Mica and minerals with high density were sorted in layers between quartz and feldspar. One could argue that the distance between quartz dissolved by mica, and fresh quartz surfaces would mostly be rather short and constant in these intervals. In this case, however, more wave sorted samples buried 3-5 km are needed to support any further assumptions.

Quartz cement was in individual samples growing around the precipitated illite. This suggests that this quartz cement postdates the precipitation of illite and/or kaolinite, and that it occurred at temperatures >130°C. Quartz cementation is however an ongoing process, so it is not uncommon to find quartz cement surrounding previously precipitated minerals.

6.2.2 Precipitation of illite

Aside from quartz and carbonate cementation, clay cementation is one of the most porosity and permeability damaging processes in the Brent Group. Precipitation of illite in the Brent sandstones is primarily a function of the amount and distribution of potassium (K^+) and temperature. Hence, the foundation for illitization can be made soon after burial when the dissolution of K-feldspars and precipitation of kaolinite occur.

As figures 5.2, 5.8 and 5.13 show, illite is present mostly in samples buried deeper than 3.5 km. This corresponds to temperatures of >130°C. A few exceptions were observed, with small quantities of illite present in shallower sandstone units. Other workers have found illite at temperatures around 90-95°C, or a depth corresponding to 3 km, on the Norwegian Shelf (Ehrenberg et al., 1993). Illite also occurs as a result of a reaction between K-feldspar and smectite (Lanson et al., 2002). Smectite is less stable than kaolinite at lower temperatures, meaning the process of illitization can start earlier in the diagenesis. Hower et al. (1976) suggests that illitization of smectite starts at around 70°C, which may explain the small quantities of illite found in samples shallower than 3.5 km.

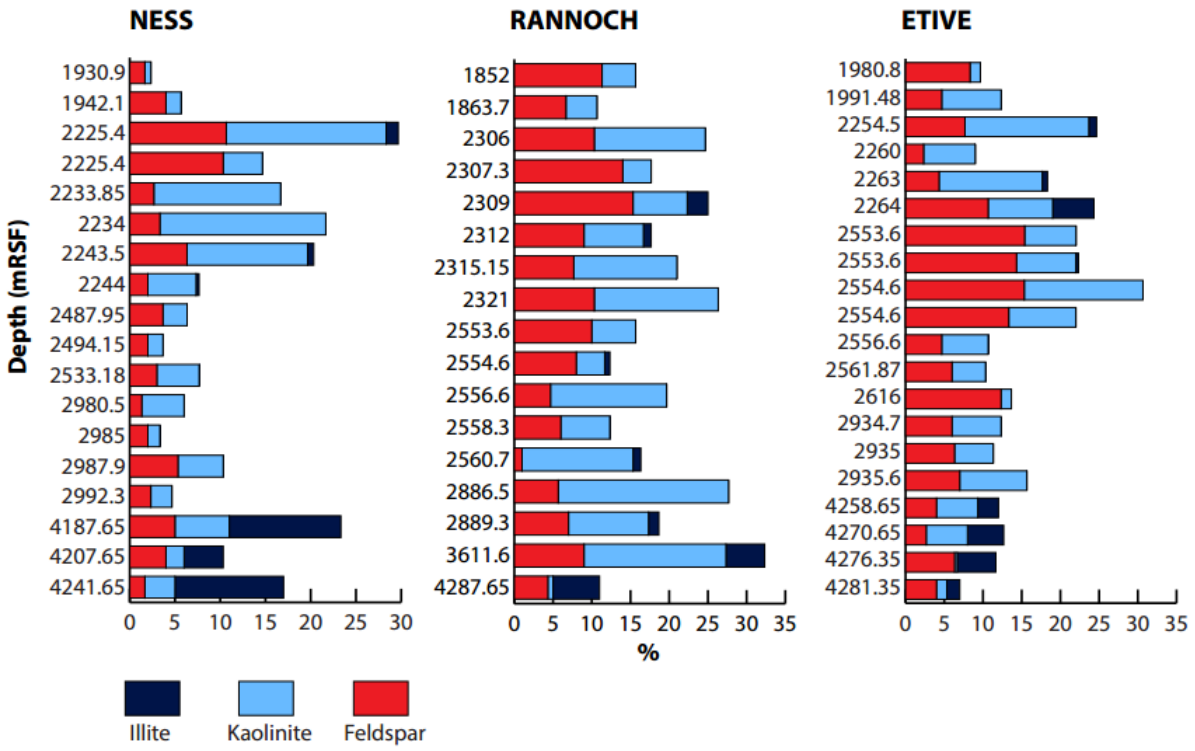

Figure 6.5: The amount of feldspar, kaolinite and illite versus depth in all three formations.

Results from the point counting imply that illite occurs more often in the Ness Formation than the Rannoch and Etive formations relative to the kaolinite content. This may be a result of the low feldspar/kaolinite ratio previously discussed. More kaolinite present at early burial means a higher potential for illitization at greater depths. This does, however, require a source of potassium such as K-feldspar adjacent to the kaolinite. It may also be the result of illitization of smectite. Infiltration of some smectite into channel sandstones during flooding of the delta flood plain may occur. The smectite will later be transformed to illite above 70°C. All the samples buried deeper than 4 km were collected from the same well, regardless of formation (well 34/10-23). In this well, the kaolinite content was higher in the Ness Formation than in the other two formations. This may also explain why we see a higher content of illite in the Ness Formation, in this particular study. To investigate this matter further, more deeply buried samples from all formations are needed.

As seen in figure 5.20a & b, the illite in the Ness Formation doesn't seem to be as pore space consuming as the illite in the Etive Formation. The illite in the Ness Formation is often observed coating the pore walls, and does not in every sample seem to have much influence on permeability. Illite is, however, more widespread in the Ness Formation than in the Etive Formation. The illite in the Etive Formation is more concentrated within certain pores. This may be a result of damaged or poorly prepared thin sections as the evidence of missing grains is substantial in some of the thin sections. Illite observed in some of well-preserved thin sections (fig. 5.23c & d) show that the illite is severely damaging the permeability in sandstones buried deeper than 3.5 km. This indicates that perhaps the amount of illite alone is not enough to determine permeability, but that distribution and location within the pores are also important factors.

The morphology of precipitated clays is a bit tricky to study in thin sections, but it is clear that the illite in many cases has a "hair-like" filamentous morphology.

Through SEM analysis, most of the feldspars present in samples buried deeper than 4 km were determined to be albite. However, there were a few exceptions. Coexisting K-feldspar and kaolinite in partly illitized sandstones is not uncommon. This has also been observed by other workers (Ehrenberg, 1991, Lanson et al., 2002). One or more reasons could explain this:

I) K-feldspar is found as inclusions in albite, and is therefore isolated from the pore-water.

II) Illitization of the outer edges of the kaolinite. This would prevent or slow down K^+ from reaching the inner kaolinite, because of the decreased permeability.

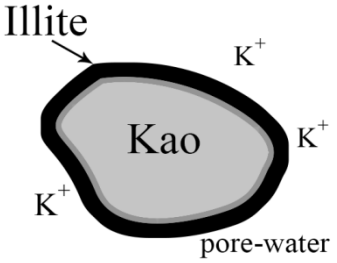

Figure 6.6: Illustration of kaolinite trapped inside illite, resulting in a reduction of illitization due to decreased permeability between the pore-water and the kaolinite.

6.2.3 Carbonate Cementation

Carbonate cementation was observed to a varying degree in all three formations. Extensive carbonate cementation was observed in thin layers at certain depths. Samples within meters of each other displayed considerable variations in degree of carbonate cementation. Although carbonate cementation is believed to occur predominantly in marine facies, extensive cementation was also observed in the more proximal Ness Formation. The carbonate cement found in the Ness Formation was mainly calcite, while the Etive and Rannoch formations are in addition associated with Mg-rich siderite and Fe-rich ankerite.

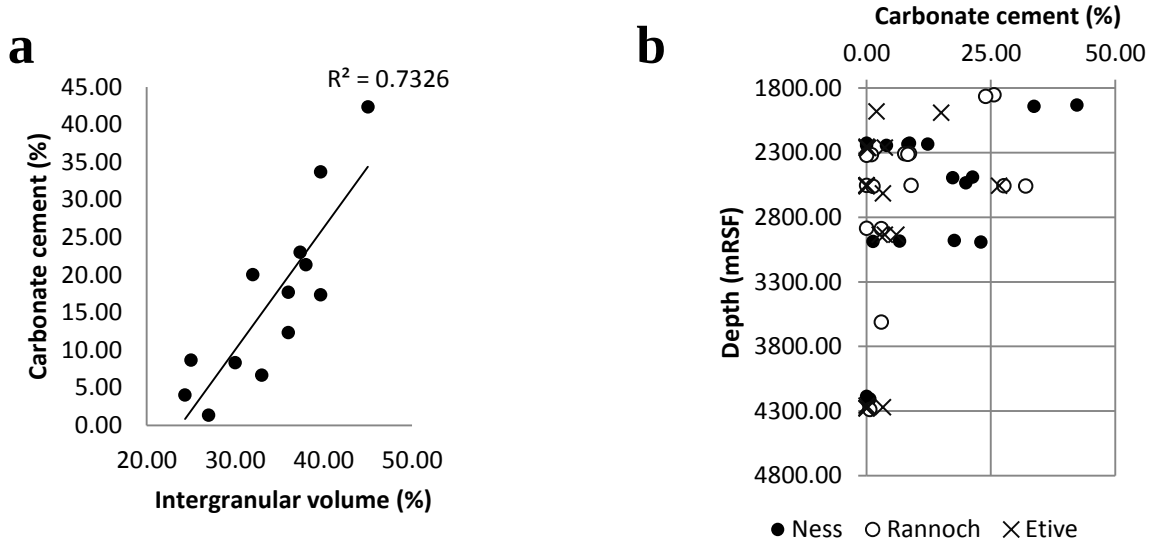

Figure 6.7: a) Correlation between carbonate cementation and intergranular volume in the Ness Formation, b) carbonate cement dissolving with depth.

The intergranular volume is fairly constant with depth, but as seen in figure 6.6, the IGV above 40% can be preserved because of carbonate cementation. The IGV is a function of several factors during mechanical compaction, such as grain size and sorting. However, since the carbonate cement is precipitated at the early stages of diagenesis, it will preserve the sediments from further mechanical compaction. The carbonate cement will severely damage the reservoir quality of the sandstone due to the decline in porosity, but it has received particular interest because cemented intervals may act as fluid migration barriers (Bjørlykke et al., 1992). The point counting suggests that carbonate cementation is less extensive in the Etive Formation, which makes it a better reservoir rock in terms of carbonate cementation.

Because of the layers of heavily carbonate cemented layers found in the Ness and Rannoch formations, it should be considered as a major diagenetic control for the Brent Group.

6.3 Minor diagenetic controls

6.3.1 Albitization of K-feldspar

Some albite was found in all three formations (i.e. fig. 5.17b & c). The low content of albite in the studied samples indicates a high degree of plagioclase leaching and possibly absence of a sufficient sodium source. Most areas of dissolved K-feldspar were dominated by either kaolinite or illite.

6.4 Intergranular volume

In the Ness and Rannoch formations, there was a slight trend of higher IGV with better sorting. In the Etive Formation, the data was inconclusive. When IGV was compared to grain sizes, no clear tendency was found in the Ness Formation. In the Etive and Rannoch formations, there was a slight trend of higher IGV with finer grain sizes. IGV showed no correlation with depth, other than a slightly higher IGV in the shallowest samples from the Rannoch Formation. These values are, however, interpreted to be a factor of carbonate cementation rather than depth.

7 Conclusions

- Petrographic analyses show a good relationship between K-feldspar, kaolinite and illite in the Brent sandstones. The amount of K-feldspar decreases with depth, when subject to albitization at intermediate depths (2-3 km) or illitization of kaolinite at deep burial (>3.5 km).

- The amount of K-feldspar and kaolinite, and their ratio, is dependent on facies. Solidified K-feldspar increase distally, allowing less kaolinite to precipitate at shallow depths. Kaolinite might, however, have been reworked into the sediments, especially in the Etive Formation.

- Smectite is likely to be the reason of illitization at temperatures <130°C, while illitization of kaolinite is dominant at temperatures >130°C.

- Carbonate cement occur in all three formations. The most heavily carbonate cemented layers were found in the Ness and Rannoch formations. The intergranular volume is preserved in the most heavily carbonate cemented samples. Porosity is severely damaged as a result. These layers may act as fluid migration barriers, trapping hydrocarbons below. They are therefore important in terms of reservoir geology.

- Quartz cement is one of the most reservoir damaging processes in all three formations.No coating of the grain surfaces was observed in the deepest buried samples (well34/10-23). The amount of quartz cement is therefore likely to higher in these samplesthan in areas of coated sediments.

References

AAGAARD, P., EGEBERG, P., SAIGAL, G., MORAD, S. & BJORLYKKE, K. 1990. Diagenetic Albitization of Detrital K-Keldspars in Jurassic, Lower Cretaceous and Tertiary Clastic Reservoir Rocks from Offshore Norway, II. Formation Water Chemistry and Kinetic Considerations. *Journal of sedimentary Research,* 60.

AAGAARD, P. & HELGESON, H. C. 1982. Thermodynamic and kinetic constraints on reaction rates among minerals and aqueous solutions; I, Theoretical considerations. *American Journal of Science,* 282**,** 237-285.

AASE, N. E., BJORKUM, P. A. & NADEAU, P. H. 1996. The effect of grain-coating microquartz on preservation of reservoir porosity. *AAPG bulletin,* 80**,** 1654-1673.

AAGAARD, P., EGEBERG, P., SAIGAL, G., MORAD, S. & BJORLYKKE, K. 1990. Diagenetic Albitization of Detrital K-Keldspars in Jurassic, Lower Cretaceous and Tertiary Clastic Reservoir Rocks from Offshore Norway, II. Formation Water Chemistry and Kinetic Considerations. *Journal of sedimentary Research,* 60.

AAGAARD, P. & HELGESON, H. C. 1982. Thermodynamic and kinetic constraints on reaction rates among minerals and aqueous solutions; I, Theoretical considerations. *American Journal of Science,* 282**,** 237-285.

ANGEVINE, C. L. & TURCOTTE, D. L. 1983. Porosity reduction by pressure solution: A theoretical model for quartz arenites. *Geological Society of America Bulletin,* 94**,** 1129-1134.

BJØRLYKKE, K. 1998. Clay mineral diagenesis in sedimentary basins—a key to the prediction of rock properties. Examples from the North Sea Basin. *Clay minerals,* 33**,** 15-34.

BJØRLYKKE, K. 2010. Compaction of Sedimentary Rocks Including Shales,Sandstones and Carbonates. *Petroleum Geoscience: from Sedimentary Environments to Rock Physics.* Springer.

BJØRLYKKE, K. 2013. Relationships between depositional environments, burial history and rock properties. Some principal aspets of diagenetic process in sedimentary basins. *Sedimentary Geology, 301, 1-14:* KNIGHT, J. (ed.). Elsevier.

BJØRLYKKE, K. & AAGAARD, P. 1992. Clay minerals in North Sea sandstones. *SEPM, Special Publication,* 47**,** 65-80.

BJØRLYKKE, K. & BRENDSDAL, A. 1986. Diagenesis of the Brent sandstone in the Statfjord field, North Sea. *The Society of Economic Paleontologists and Mineralogist,* Roles of Organic Matter in Sediment Diagenesis (SP38).

BJORLYKKE, K. & EGEBERG, P. 1993. Quartz cementation in sedimentary basins. *AAPG bulletin,* 77**,** 1538-1548.

BJØRLYKKE, K. & JAHREN, J. 2010. Sandstones and Sandstone Reservoirs. *Petroleum Geoscience: from Sedimentary Environments to Rock Physics.* Berlin: Heidelberg: Springer-Verlag Berlin Heidelberg.

BJØRLYKKE, K., NEDKVITNE, T., RAMM, M. & SAIGAL, G. C. 1992. Diagenetic processes in the Brent Group (Middle Jurassic) reservoirs of the North Sea: an overview. *Geological Society, London, Special Publications,* 61**,** 263-287.

BJØRLYKKE, K. & JAHREN, J. 2010. Sandstones and Sandstone Reservoirs. *Petroleum Geoscience: from Sedimentary Environments to Rock Physics.* Berlin: Heidelberg: Springer-Verlag Berlin Heidelberg.

CHRISTIANSSON, P., FALEIDE, J. & BERGE, A. 2000. Crustal structure in the northern North Sea: an integrated geophysical study. *SPECIAL PUBLICATION-GEOLOGICAL SOCIETY OF LONDON,* 167**,** 15-40.

CHUHAN, F. A., KJELDSTAD, A., BJØRLYKKE, K. & HØEG, K. 2003. Experimental compression of loose sands: relevance to porosity reduction during burial in sedimentary basins. *Canadian Geotechnical Journal,* 40**,** 995-1011.

EHRENBERG, S. 1993. Preservation of anomalously high porosity in deeply buried sandstones by grain-coating chlorite: examples from the Norwegian continental shelf. *AAPG Bulletin,* 77**,** 1260-1286.

EHRENBERG, S., AAGAARD, P., WILSON, M., FRASER, A. & DUTHIE, D. 1993. Depth-dependent transformation of kaolinite to dickite in sandstones of the Norwegian continental shelf. *Clay Minerals,* 28**,** 325-352.

EHRENBERG, S. & NADEAU, P. 1989. Formation of diagenetic illite in sandstones of the Garn Formation, Haltenbanken area, mid-Norwegian continental shelf. *Clay Minerals,* 24**,** 233-253.

EHRENBERG, S. N. 1991b. Kaolinized, potassium-leached zones at the contacts of the Garn Formation, Haltenbanken, mid-Norwegian continental shelf. *Marine and Petroleum Geology,* 8**,** 250-269..

EMERY, D., MYERS, K. J. & YOUNG, R. 1990. Ancient subaerial exposure and freshwater leaching in sandstones. *Geology,* 18**,** 1178-1181.

ESLINGER, E. & PEVEAR, D. R. 1988. *Clay minerals for petroleum geologists and engineers,* Society of Economic Paleontologists and Mineralogis ts.

FALEIDE, J. I., BJØRLYKKE, K. & GABRIELSEN, R. H. 2010. Geology of the Norwegian Continental Shelf. *Petroleum Geoscience: From SedimentaryEnvironments to Rock Physics.* Springer.

FJELDSKAAR, W., TER VOORDE, M., JOHANSEN, H., CHRISTIANSSON, P., FALEIDE, J. I. & CLOETINGH, S. A. P. L. 2004. Numerical simulation of rifting in the northern Viking Graben: the mutual effect of modelling parameters. *Tectonophysics,* 382**,** 189-212.

FOLK, R. L. 1968. *Petrology of sedimentary rocks: The University of Texas Geology 370 K, 383 L, 383 M,* Austin, Texas, Hemphill`s.

GEOSCIENCEWORLD 2014. *By:* CASSAGNABERE, A. (ed.). URL: http://claymin.geoscienceworld.org/content/46/1/1/F2.large.jpg.

HALLAM, A. 1988a. A re-evaluation of Jurassic eustasy in the light of new data and the revised Exxon curve. *Wilgus, CK, Hastings, BS, Kendall, cG, Posamentier, HW., Ross, CA, Van Wagoner, Jc (Eds.), Sea-level changes: an integrated approach. Soc. Econ. Paleontol. Mineral. Spec. Publ,* 42**,** 26.

HAQ, B. U., HARDENBOL, J. & VAIL, P. R. 1987. Chronology of fluctuating sea levels since the Triassic. *Science,* 235**,** 1156-1167.

HOWER, J., ESLINGER, E. V., HOWER, M. E. & PERRY, E. A. 1976. Mechanism of burial metamorphism of argillaceous sediment: 1. Mineralogical and chemical evidence. *Geological Society of America Bulletin,* 87**,** 725-737.

JENNETTE, D. C. & RILEY, C. O. 1996. Influence of relative sea-level on facies and reservoir geometry of the Middle Jurassic lower Brent Group, UK North Viking Graben. *Geological Society, London, Special Publications,* 104**,** 87-113.

JOHANNESSEN, E. P. & NØTTVEDT, A. 2006. Norge omkranses av kystsletter og deltaer. *Landet blir til, Norges geologi.* Trondheim: Norsk geologisk forening.

KITTILSEN, J. E. 1987. *Sandproduksjon fra oljereservoarer belyst ved en sedimentologisk og diagenetisk undersøkelse av materiale fra Statfjordfeltet.* Cand. Scient, University of Oslo.

LAND, L. S. & DUTTON, S. P. 1978. Cementation of a Pennsylvanian Deltaic Sandstone: Isotopic Data. *Journal of Sedimentary Petrology,* 48**,** 1167-1176.

LANSON, B., BEAUFORT, D., BERGER, G., BAUER, A., CASSAGNABERE, A. & MEUNIER, A. 2002. Authigenic kaolin and illitic minerals during burial diagenesis of sandstones: a review. *Clay Minerals,* 37**,** 1-22.

LEDER, F. & PARK, W. C. 1986. Porosity Reduction in Sandstone by Quartz Overgrowth. *American Association of Petroleum Geologists,* 70**,** 1713-1728.

MCBRIDE, E. F. 1989. Quartz cement in sandstones: a review. *Earth-Science Reviews,* 26**,** 69-112.

MILTON, T. H. 1955. Stylolites in Sandstones. *The Journal of Geology,* 63**,** 101-114.

MITCHENER, B., LAWRENCE, D., PARTINGTON, M., BOWMAN, M. & GLUYAS, J. 1992. Brent Group: sequence stratigraphy and regional implications. *Geological Society, London, Special Publications,* 61**,** 45-80.

MOORE, C. H. 1989. *Carbonate diagenesis and porosity,* Elsevier.

NESSE, W. D. 2004. Introduction to optical mineralogy.

NORLEX 2014. Lithostratigraphic chart, offshore Norway.

NPD.NO 2014. Fact Maps. npd.no: Norwegian Petroleum Directorate.

OLSEN, T. R. & STEEL, R. J. 2000. The significance of the Etive Formation in the development of the Brent system: distinction of normal and forced regressions. *Geological Society, London, Special Publications,* 172**,** 91-112.

REYNOLDS, A. D. 1995. Sedimentology and sequence stratigraphy of the thistle field, northern north sea. *In:* R.J. STEEL, V. L. F. E. P. J. & MATHIEU, C. (eds.) *Norwegian Petroleum Society Special Publications.* Elsevier.

RICHARDS, P. C. 1992. An introduction to the Brent Group: a literature review. *Geological Society, London, Special Publications,* 61**,** 15-26.

SAIGAL, G. C., MORAD, S., BJORLYKKE, K., EGEBERG, P. K. & AAGAARD, P. 1988. Diagenetic albitization of detrital K-feldspar in Jurassic, Lower Cretaceous, and Tertiary clastic reservoir rocks from offshore Norway, I. Textures and origin. *Journal of Sedimentary Research,* 58.

SURLYK, F. 1991. Sequence Stratigraphy of the Jurassic-Lowermost Cretaceous of East Greenland (1). *AAPG Bulletin,* 75**,** 1468-1488.

SZABO, J. & PAXTON, S. 1991. Intergranular volume (IGV) decline curves for evaluating and predicting compaction and porosity loss in sandstones. *AAPG Bulletin (American Association of Petroleum Geologists);(United States),* 75.

TADA, R. & SIEVER, R. 1989. Pressure Solution during Diagenesis. *Annual Review of Earth and Planetary Sciences,* 17.

VELDE, B. 1995. *Origin and mineralogy of clays: clays and the environment,* Berlin, Springer.

VOLLSET, J. & DORÉ, A. G. 1984. A revised Triassic and Jurassic lithostratigraphic nomenclature for the Norwegian North Sea: Norwegian Petroleum Directorate Bulletin. 3.

YIELDING, G., BADLEY, M. E. & ROBERTS, A. M. 1992. The structural evolution of the Brent Province. *Geological Society, London, Special Publications,* 61**,** 27-43.

WALDERHAUG, O. 1994. Temperatures of quartz cementation in Jurassic sandstones from the Norwegian continental shelf--evidence from fluid inclusions. *Journal of Sedimentary Research,* 64.

WALDERHAUG, O. 1996. Kinetic Modeling of Quartz Cementation and Porosity Loss in Deeply Buried Sandstone Reservoirs. *The American Association of Petroleum Geoligists* 80**,** 731-745.

WALDERHAUG, O. & BJORKUM, P. A. 2003. The Effect of Stylolite Spacing on Quartz Cementation in the Lower Jurassic Sto Formation, Southern Barents Sea. *Journal of Sedimentary Research,* 73**,** 146-156.

WEAVER, C. E. 1989. *Clays, muds, and shales,* Elsevier.

WORDEN, R. & MORAD, S. 2000. Quartz cementation in oil field sandstones: a review of the key controversies. *Quartz cementation in sandstones,* 29**,** 1-20.

XIAOCHI, L. & GRANT-MACKIE, J. 1993. Jurassic sedimentary cycles and eustatic sea-level changes in southern Tibet. *Palaeogeography, palaeoclimatology, palaeoecology,* 101**,** 27-48.

YIELDING, G., BADLEY, M. E. & ROBERTS, A. M. 1992. The structural evolution of the Brent Province. *Geological Society, London, Special Publications,* 61**,** 27-43.